Gulf of California and Rio Grande Rifts

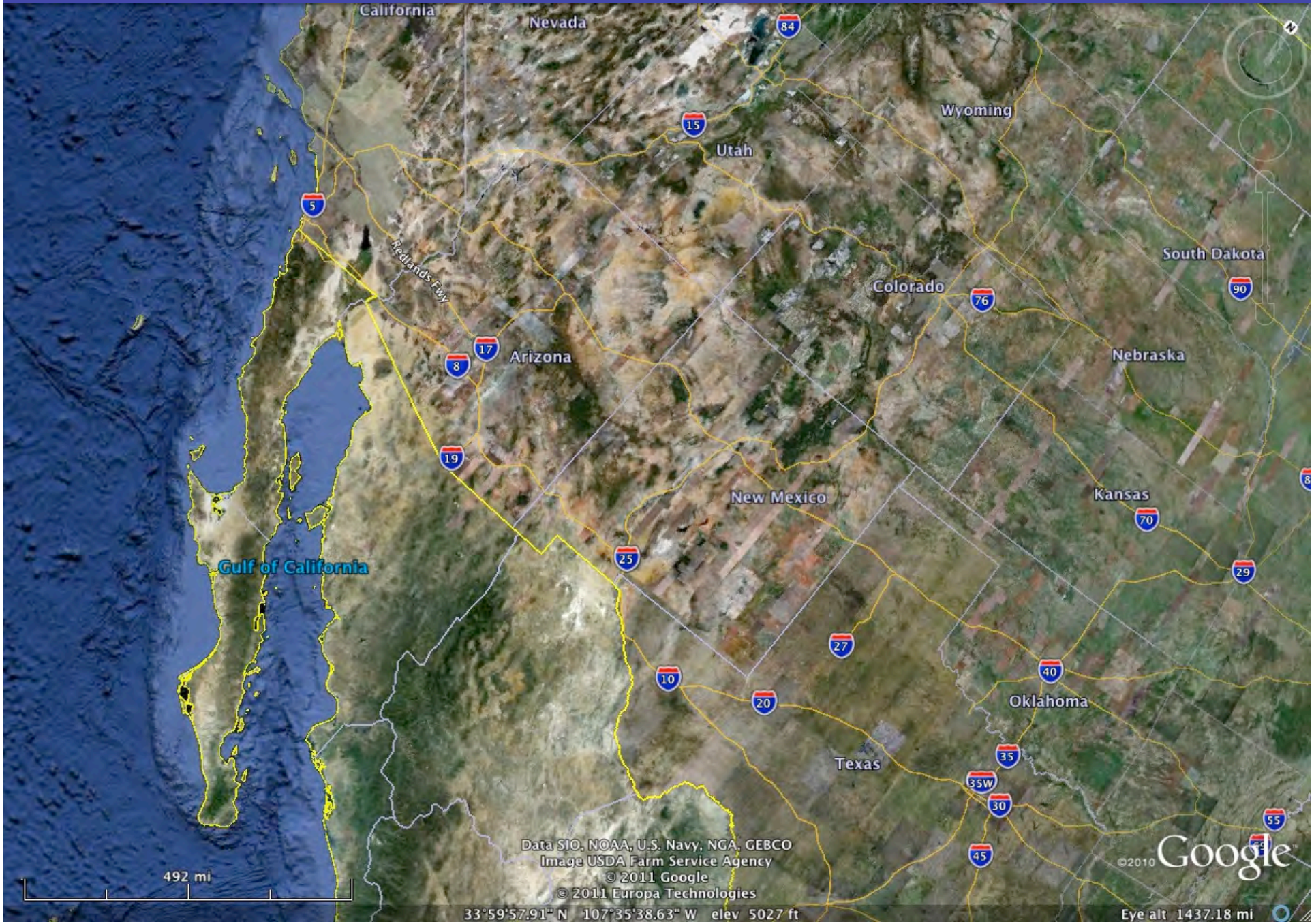

ISS018E005084

ISS006E19024

ISS014E08306

ISS014E15392

Puerta Vallarta

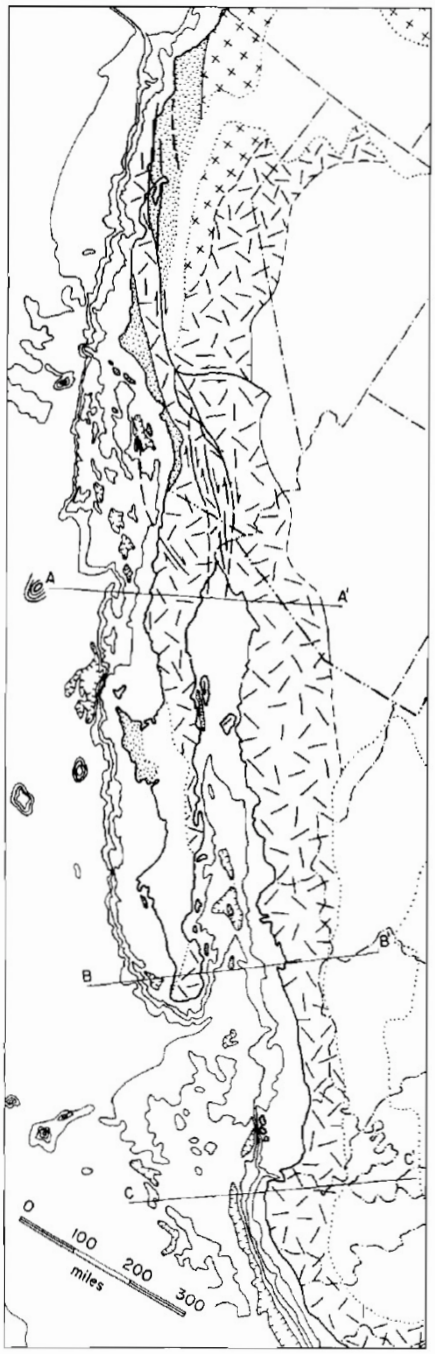

EXPLANATION

Franciscan terrane (Jurassic and Cretaceous eugeosynclinal rocks)

Terrane metamorphosed regionally and intruded by batholiths during Cretaceous time. (Extent uncertain in mainland Mexico)

Nevadan orogen (Terrane metamorphosed regionally and intruded by stocks during Jurassic time)

Major known strike-slip faults

Boundary of area from which no data are available

A A'
Line of section (Figure 4)

Figure 2. Map of major pre-Tertiary rock complexes of California and Pacific Coast region of Mexico. Submarine contour interval 1000 m

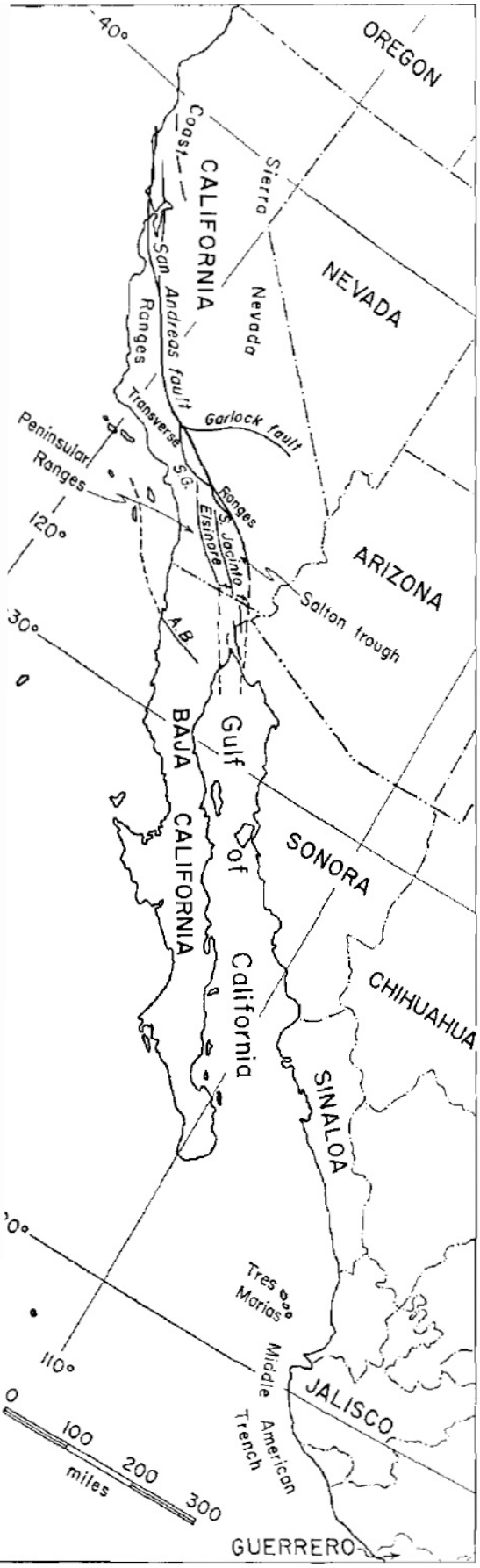

gure 1. Map of California and Pacific Coast region of Mexico. S. G., San Gabriel fault; A. B., Agua Blanca fault

Hamilton 1961
The Origin of the Gulf of California
GSA Bulletin

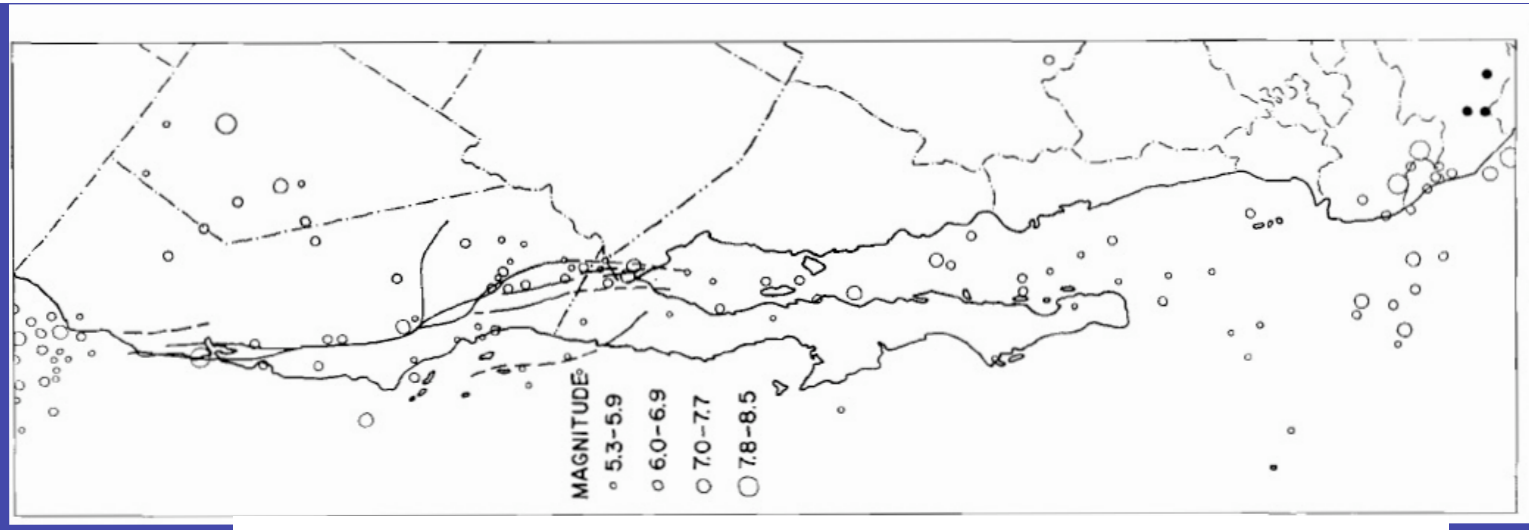

igure 3. Epicenters of earthquakes in California and Pacific Coast region of Mexico. Open circles, depth shallower than 60 km; solid circles, depth greater than 70 km. After Gutenberg and Richter (1954, Figs. 8, 9)

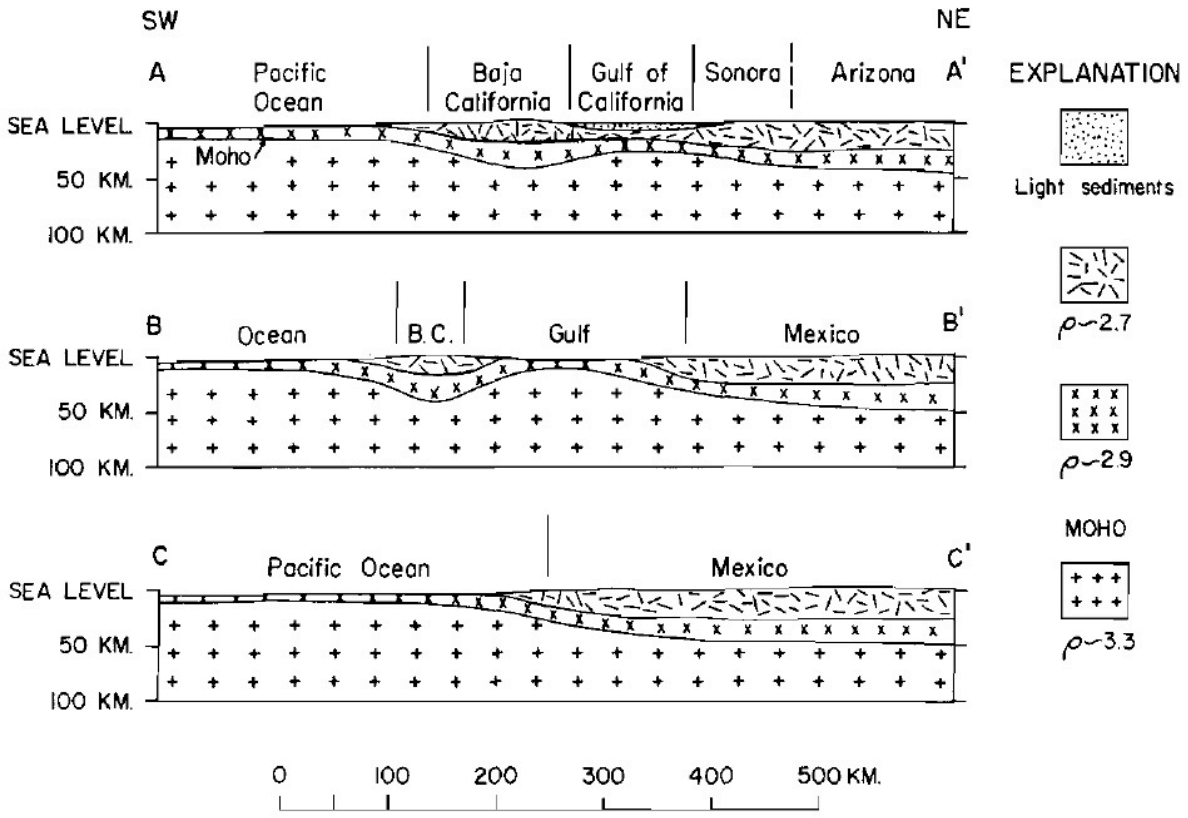

Figure 4. Schematic sections of crustal structure in Gulf of California region. Locations shown on Figure 2. No vertical exaggeration

Pacific Ocean, and a number of geologists and geophysicists (as for example, Benioff, 1959) have suggested that the ocean basin is rotating counterclockwise relative to the continents. Earthquake first-motion studies suggest a dominance of strike-slip movements along the

Oblique tensional rifting may be a common process. Left-lateral strike-slip faults trend from the Dead Sea trough into the long and narrow Red Sea, which has an oceanic structure like that of the Gulf of California; if the origin is similar, then Africa is moving relatively

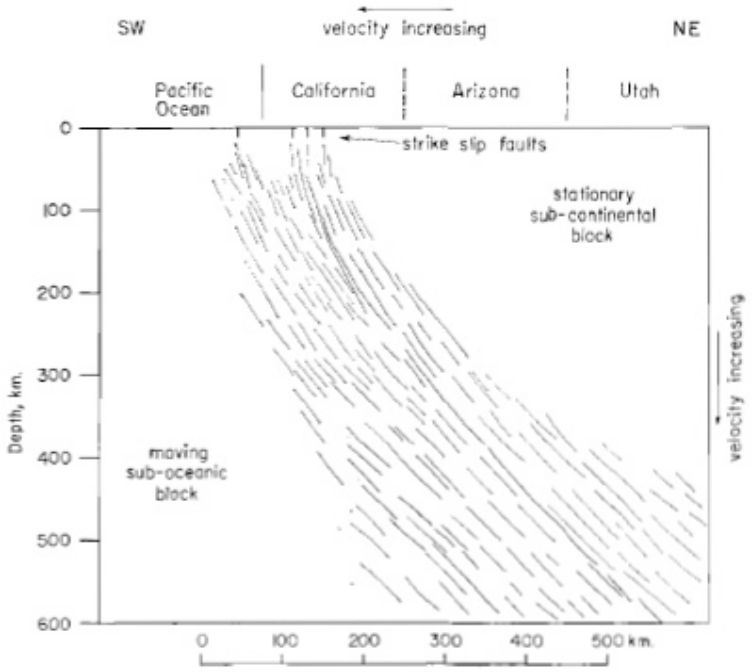

Figure 5. Cross section showing possible orientation of planes of laminar flow beneath the San Andreas fault system. Motion largely strike slip, perpendicular to the plane of the section

structures which dip beneath the island arcs and the continental margins along the ocean trenches. The mechanism of San Andreas faulting inferred in Figure 5 could produce both ocean trenches and continental strike-slip fault systems as parts of a continuous movement system. Continuity between trenches and strike-slip faults can be inferred in other places about the Pacific: for example, the Alpine fault of New Zealand, which has a right-lateral displacement comparable to that of the San Andreas fault, probably trends into theTonga Trench.

southward away from Asia Minor and the Arabian Peninsula. The Cayman Deep in the West Indies may be another tensional rift, and the Snake River depression of southern Idaho is perhaps a rift still in an early stage. Many other examples could be cited. The possibility of great lateral transport and rotation of continents and ocean basins, and of any portions of each, adds disconcerting variables to structural interpretations but provides a way to resolve the increasingly perplexing problems which are insoluble with the conventional assumption that lateral shift is of little consequence.

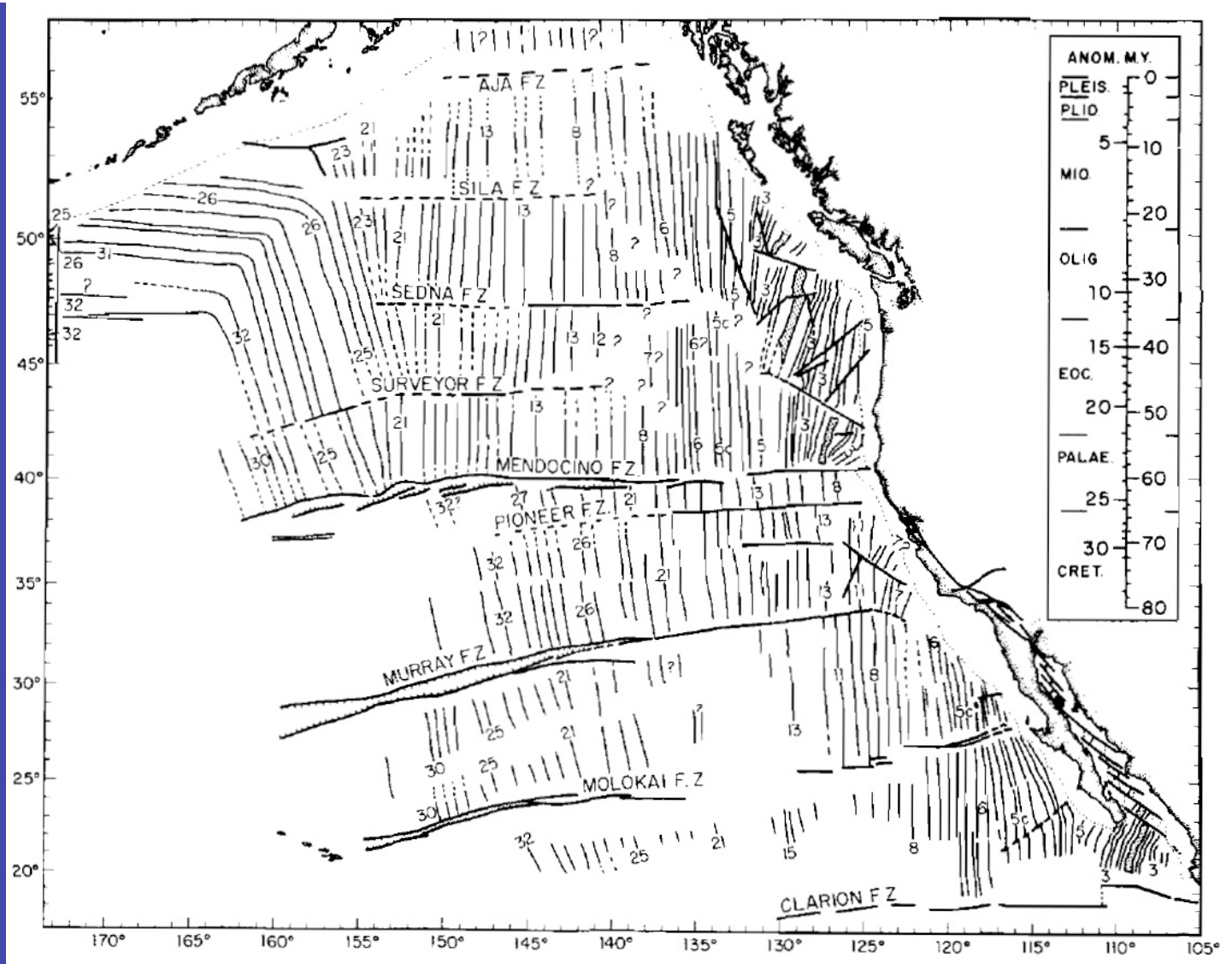

Figure 1. Magnetic anomalies in the northeast Pacific from Atwater and Menard (1970). Numbering of anomalies and their ages shown in the scale follow Heirtzler and others (1968); ages of geologic epochs follow Berggren (1969).

Atwater 1970 Implications of Plate Tectonics for the Cenozoic Evolution of Western North America *GSA Bulletin*

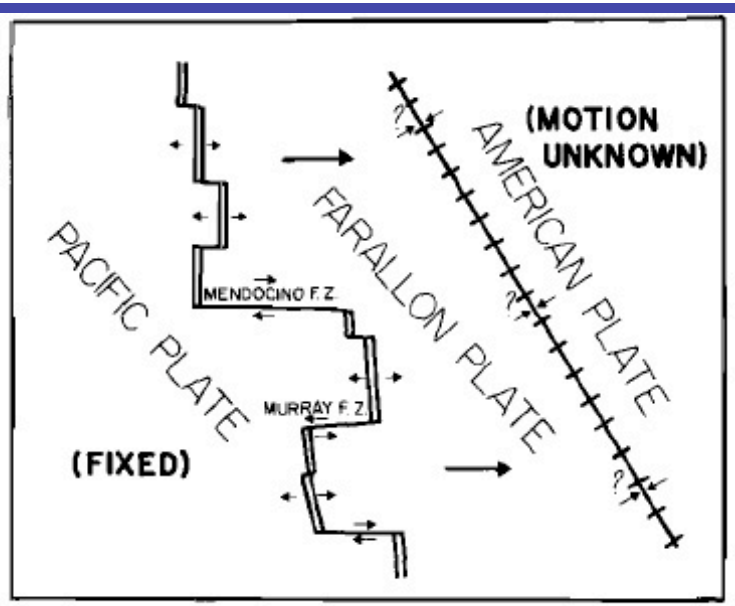

Figure 2. Configuration of plate boundaries at the time of anomaly 21, about 53 m.y. ago, as deduced from Figure 1. Magnetic anomalies and fracture zones are being created by the ridges and transform faults between 2 rigid oceanic plates. In this and subsequent figures, symbols follow McKenzie and Parker (1967): single lines are transform faults, double lines are spreading centers, and hatched lines are zones of subduction (usually trenches). Large arrows show motions of plates with respect to the Pacific plate which is arbitrarily held fixed. Small arrows show relative motions at points along plate boundaries.

are for the most part missing. This geometry indicates that there once was another plate lying to the east of the ridge, the "Farallon plate" of McKenzie and Morgan (1969), which contained the missing anomalies, and since most of this plate no longer exists, there must have been a trench which consumed it at its boundary with the American plate. This trench

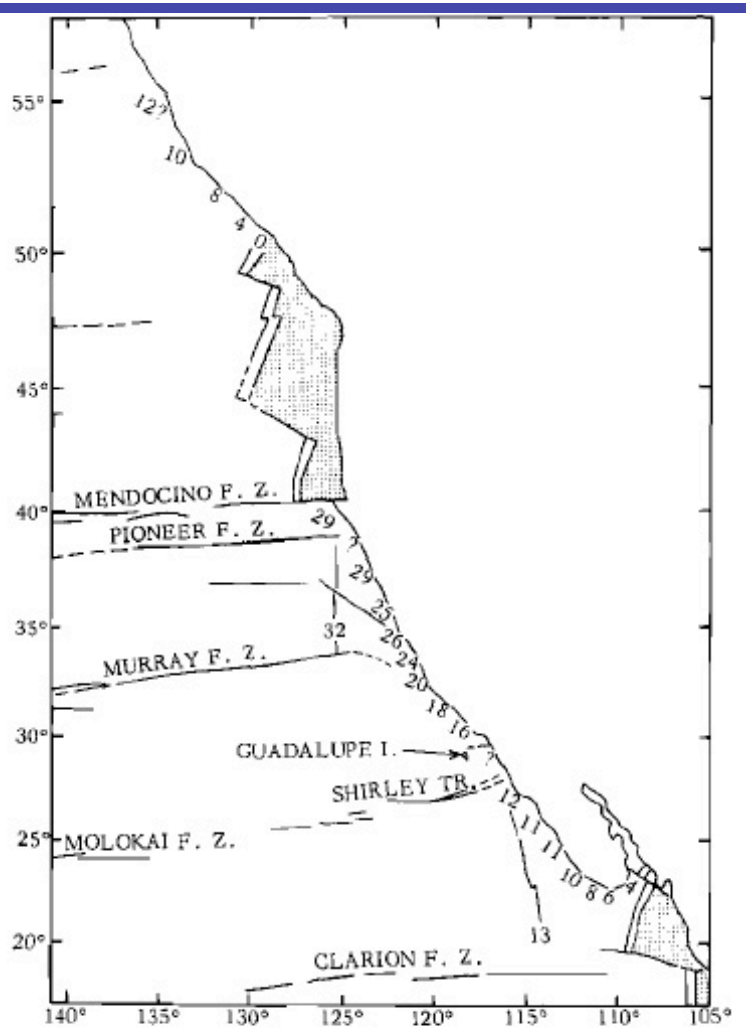

Figure 3. Ages (in millions of years before present) of easternmost recognizable anomalies in the Pacific plate. These ages indicate the earliest possible time that the ridge and trench collided and the Farallon plate was destroyed in a given region. Ceasing of trench activity and the starting of motion related to the San Andreas fault may be indicated by these ages. The coastline has been omitted to emphasize that the position of the North American plate during most of the collisions in unknown.

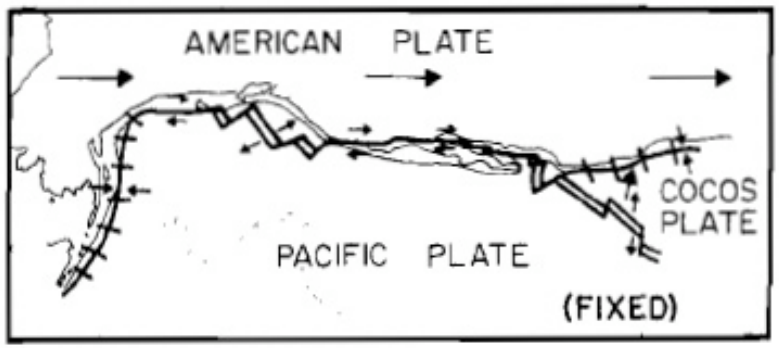

Figure 4. Present configuration of plate boundaries in the northeast Pacific and western North America, after Morgan (1968a). The map is a Mercator projection about the pole of relative motion between the Pacific and American plates, 53° N., 53° W., Morgan (1968a). Transform faults between the two plates lie on small circles about the pole of relative motion; thus, in this projection they form horizontal lines. Gray line marks the location of anomaly 21, used in Figure 2. Boundary symbols and arrows are as described in Figure 2.

of southern Baja California (Chase and others, 1970).

All of these ages supply only upper limits for the time when the trench ceased activity, for it is possible that younger anomalies once existed offshore and subsequently were overridden by the continent. It should also be emphasized that these anomalies lie within the Pacific plate and move with it. The geometrical relationship between the events they date and events on the continent cannot be deciphered until the relative motion of the North American plate is

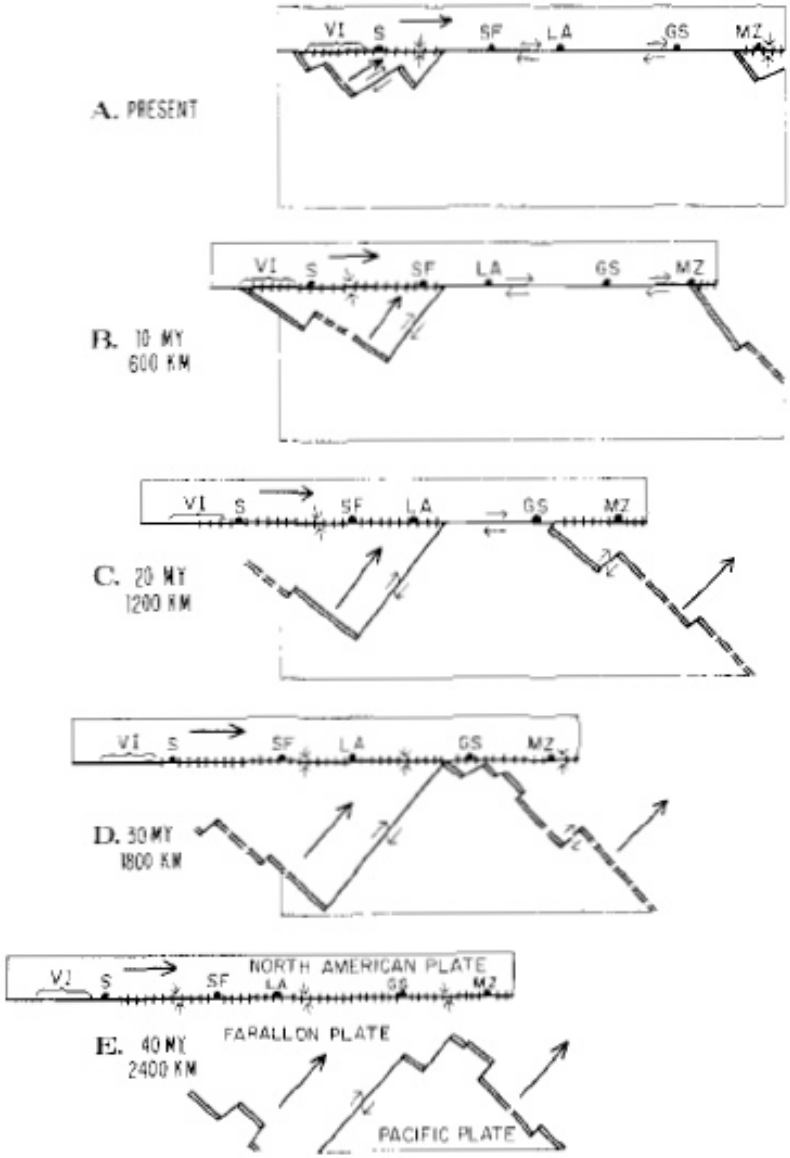

Figure 5. Schematic model of plate interactions assuming that the North American and Pacific plates moved with a constant relative motion of 6 cm/yr parallel to the San Andreas fault. The coast is approximated as parallel to the San Andreas. Farallon-

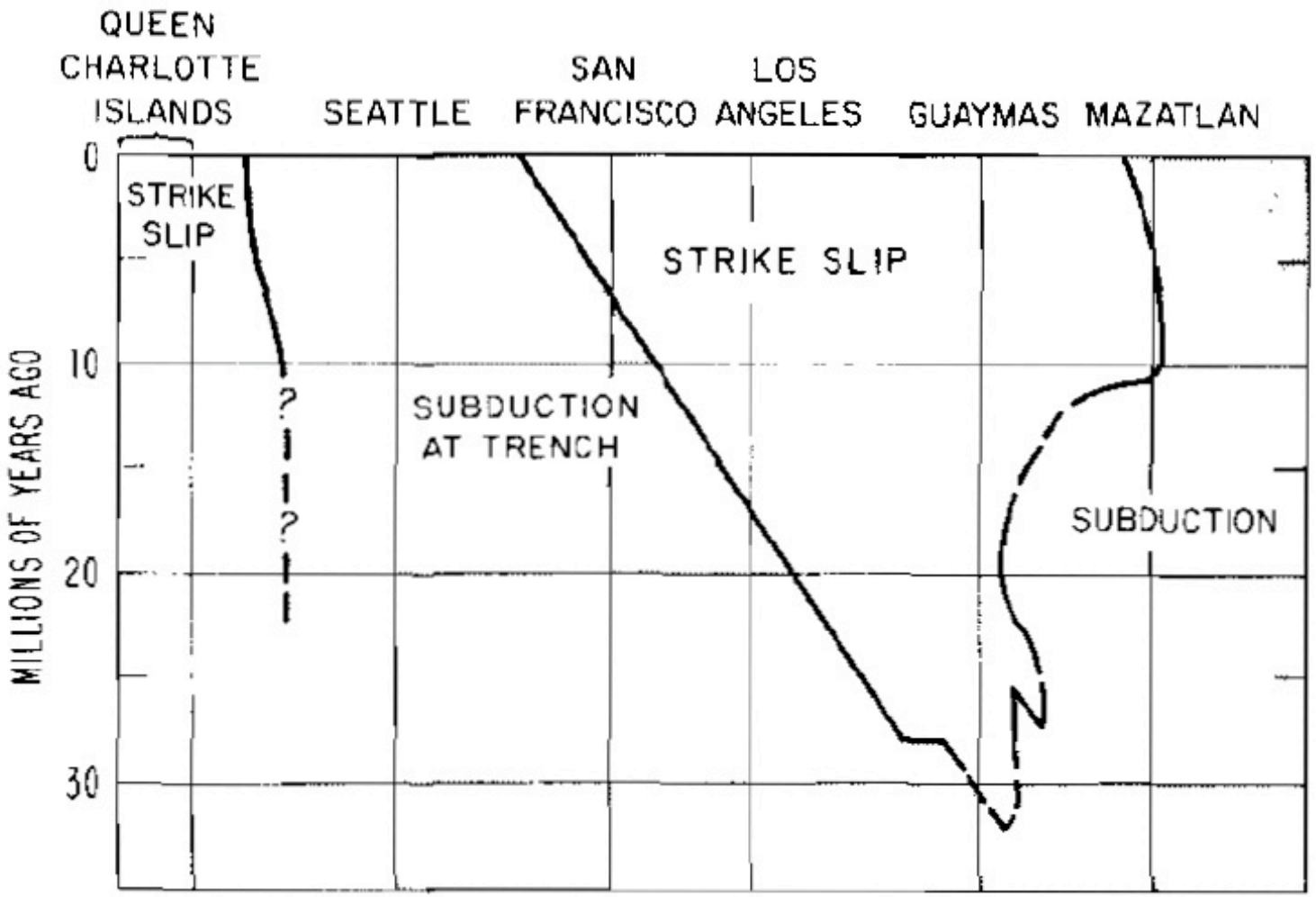

Figure 6. Evolution with time of boundary regimes along the coast of North America assuming the model of constant American-Pacific motion described in Figure 5. White areas denote times and coastal locations

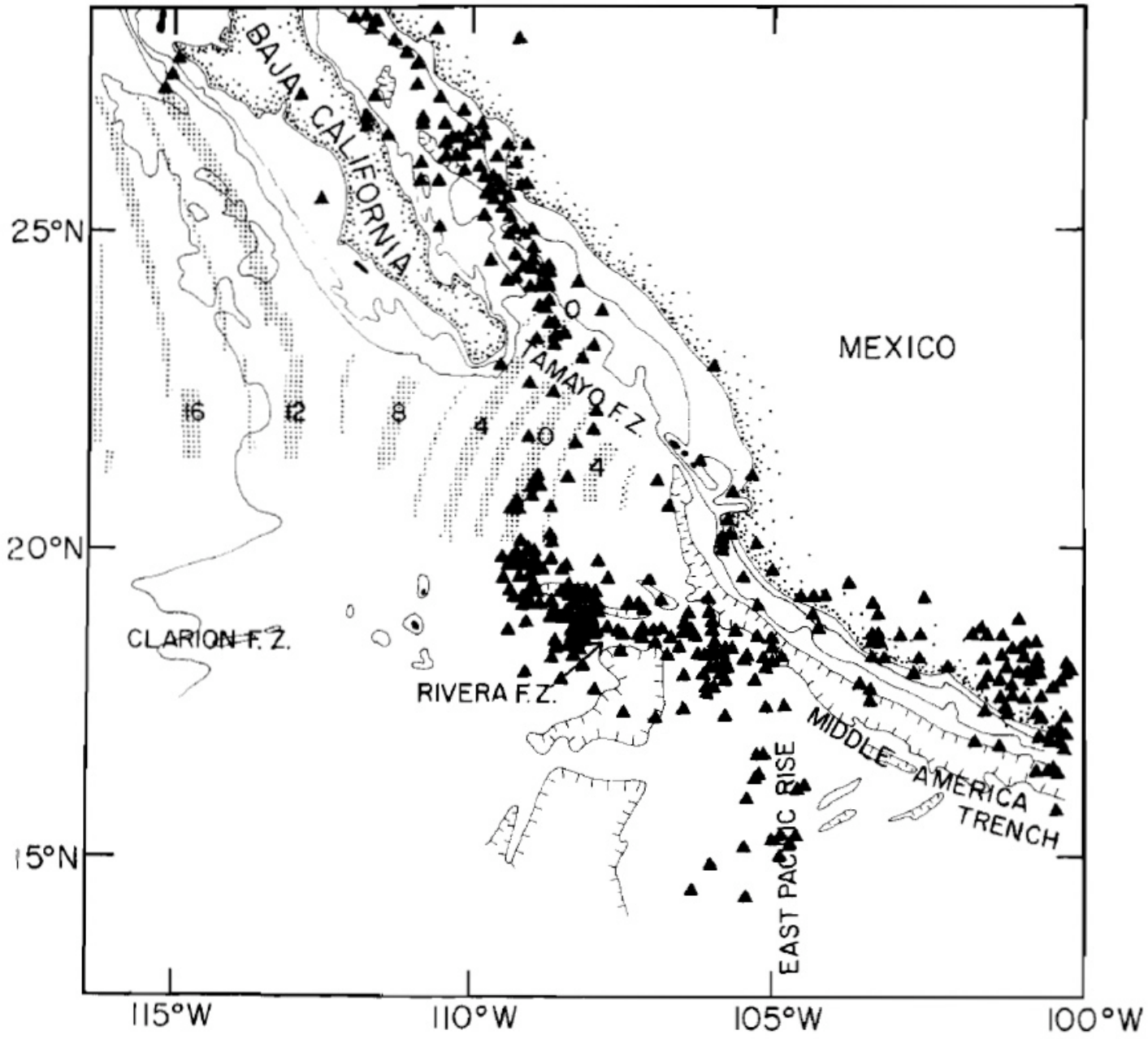

Figure 9A. Earthquake epicenters and sea-floor age near the mouth of the Gulf of California. Earthquakes (triangles) include all preliminary determinations of hypocenters of the USCGS, ESSA, between 1961 and 1967. Sea-floor ages (in millions of years before present) were deduced from anomalies as described in Larson and others (1968) and Chase and others (1970). Contours of 200, 1000, and 2000 fathoms are from Chase and Menard (1965).

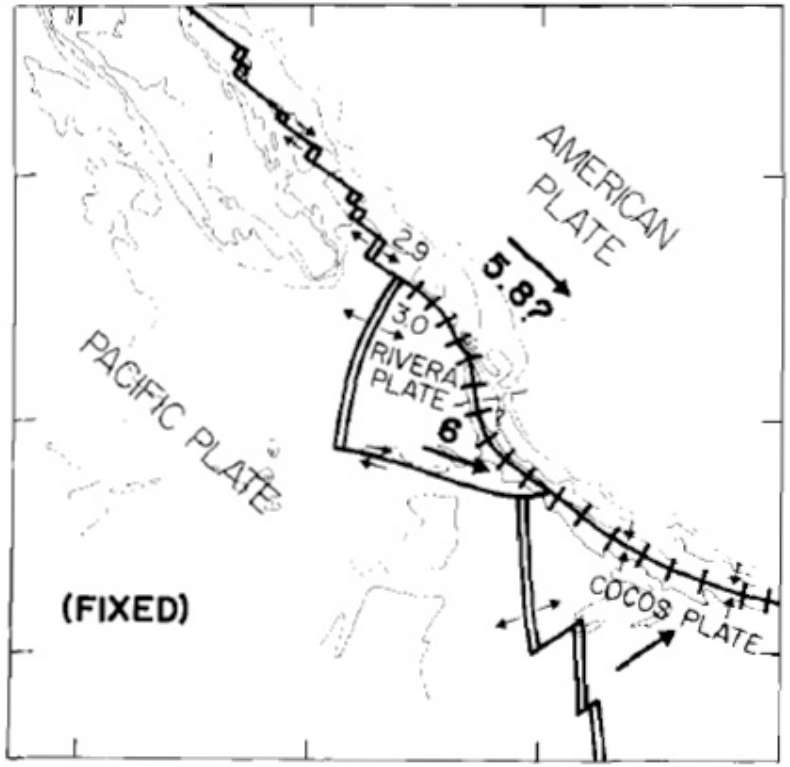

Figure 9B. Present plate configurations and motions near the mouth of the Gulf of California. Spreading rates and ridge orientation indicate that the Rivera plate may be moving approximately with the American plate; however, earthquakes, the topographic trench, and the difference in orientation of the fracture zones may be indications of compression between these two plates.

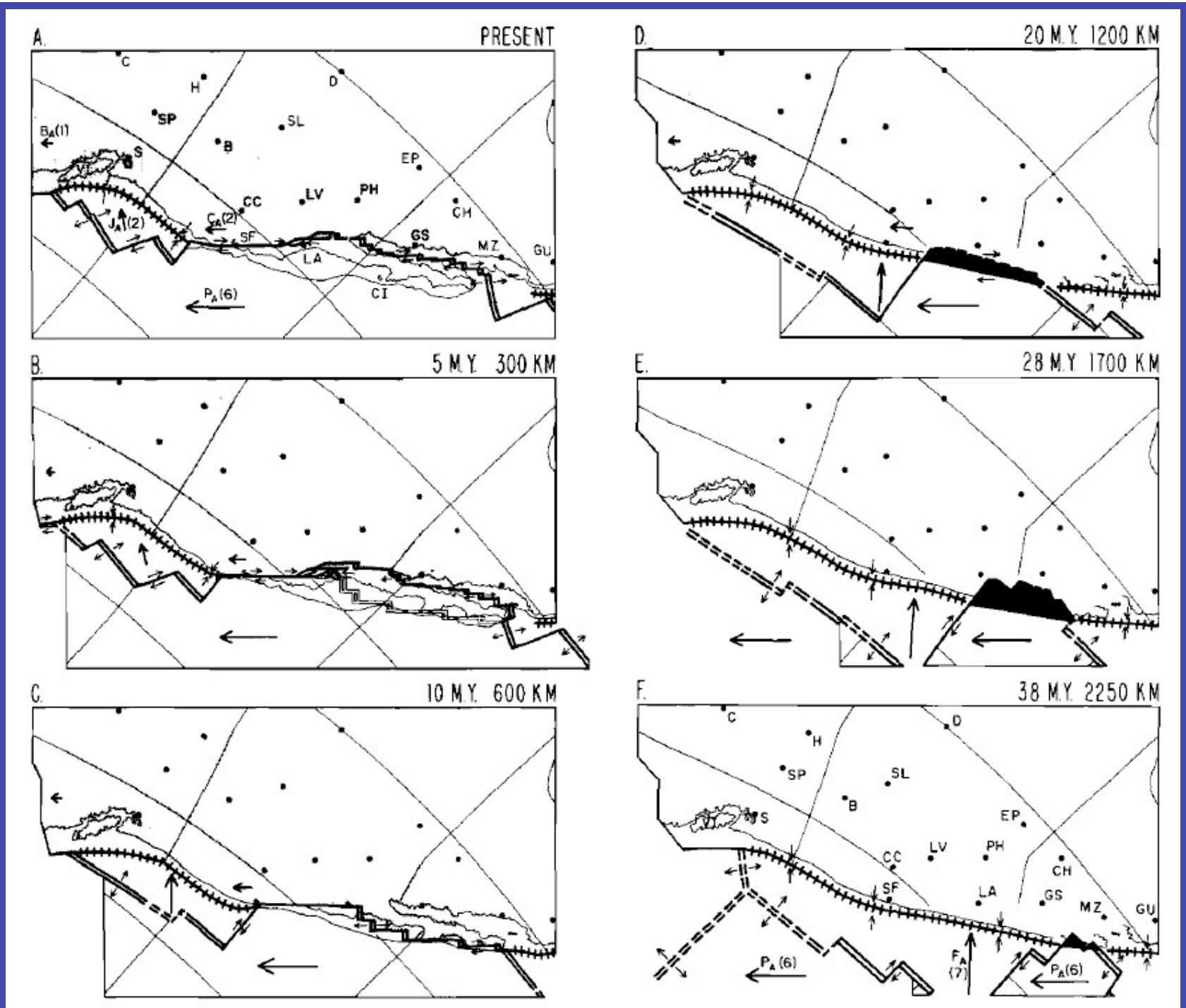
A.
PRESENT
C
H
D
SP
SL
B
S
EP
CH
CC
LV
PH
SF
LA
GS
MZ
GU
CI
B. 5 M.Y. 300 KM
C. 10 M.Y. 600 KM
D. 20 M.Y. 1200 KM
E. 28 M.Y. 1700 KM
F. 38 M.Y. 2250 KM

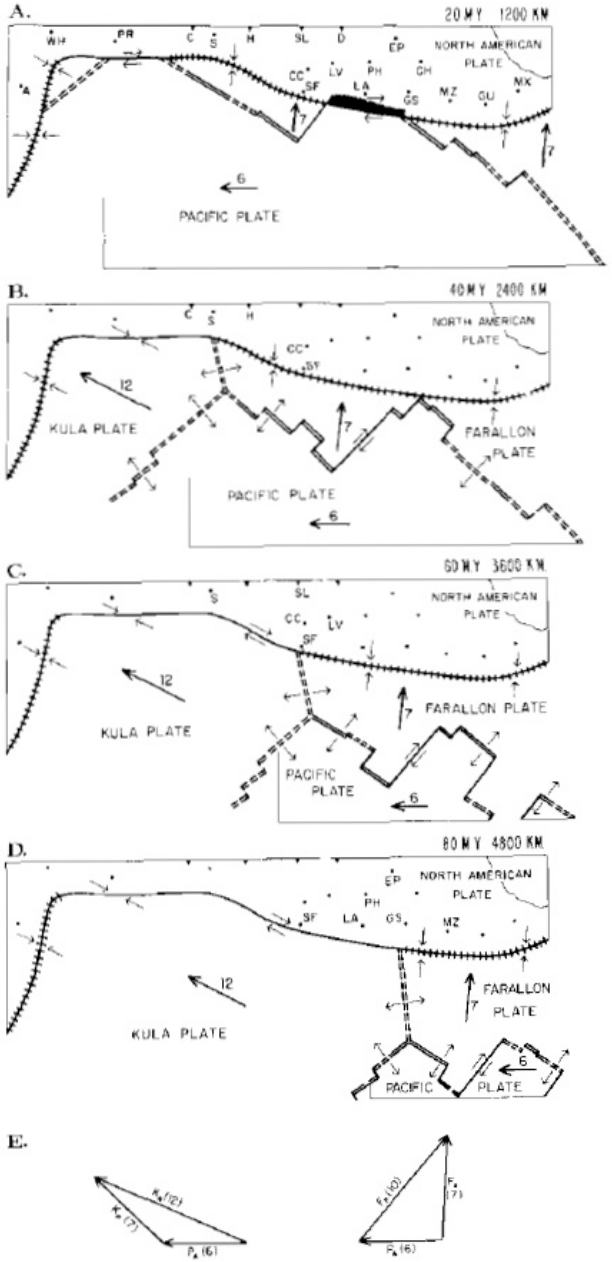

Figure 18. Plate relationships derived from extrapolation of Pacific-North American and Pacific-Kula motions through the Cenozoic. Conventions and assumptions are as in Figure 16.

Probably the most important contribution of Figure 18 is that it emphasizes the inconstant nature of plate tectonic boundary effects. The figure was constructed assuming constant relative motions of the plates, and yet, 3 different successive boundary regimes are predicted at many points along the coast.

DISCUSSION

The conclusions in the 3 main sections of this paper represent 3 different levels of uncertainty. All assume that the basic principles of sea-floor spreading and plate tectonics are approximately correct. Given this assumption, the conclusions in the first section—that a mid-Tertiary trench lay off western North America and that the San Andreas fault began activity in its present role not earlier than 30 m.y. ago—are nearly inescapable. The conclusions in the second section depend upon which model is assumed for the history of motions of the North American plate with respect to the oceanic plates. Most of the discussions and reconstructions (Figs. 5, 6, 16, and 17) in this section assume that the motions were approximately constant during the late Tertiary. Although this model appears to be the most probable one, it cannot be definitely established. The third section deals with an outrageous extrapolation of the constant motion model. Its value lies mainly in that it presents the most straightforward model for early Tertiary plate motions, and thus may serve as a starting point for discussions of plate reconstructions of that era.

ACKNOWLEDGMENTS

I am particularly indebted to H. W. Menard under whose guidance and enthusiasm this

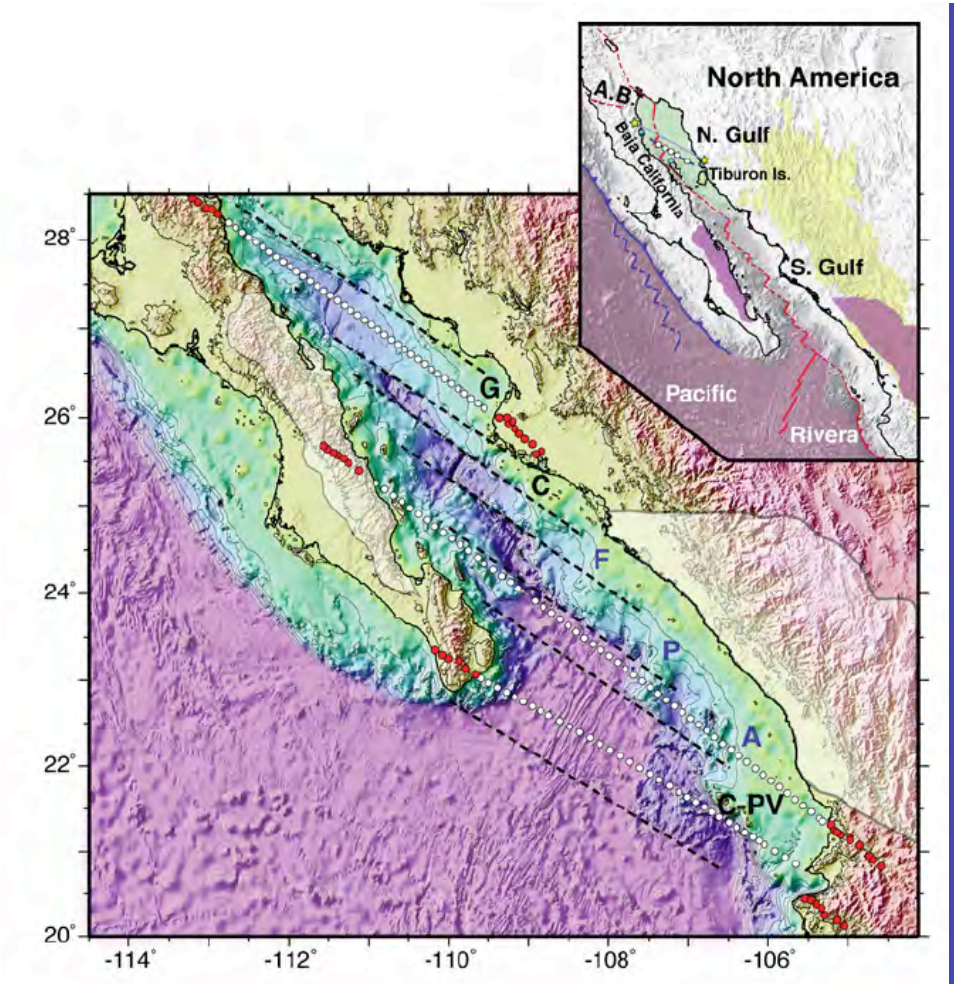

Figure 1. Map of the PESCADOR experiment in southern Gulf of California. Guaymas, Carmen, Farallón, Pescadero, Alarcón, and San José del Cabo-Puerto Vallarta segments separated by dashed lines and labelled G, C, F, P, A, C-PV, blue for south-central segments; white and red dots are instrument locations of the three seismic transects; white shading indicates extent of early Miocene ignimbrite volcanism[21]. *Inset:* Green shading, northern; pink, EPR-sourced crust; extinct and modern plate boundaries in blue and red; A.B., Agua Blanca; white and blue dots, CORTES-P96[14] instruments; geologic constraints on northern gulf spreading[27] indicated by yellow stars; and mapped extent[21] of Oligicene (yellow shading) and early Miocene (purple) ignimbrite events.

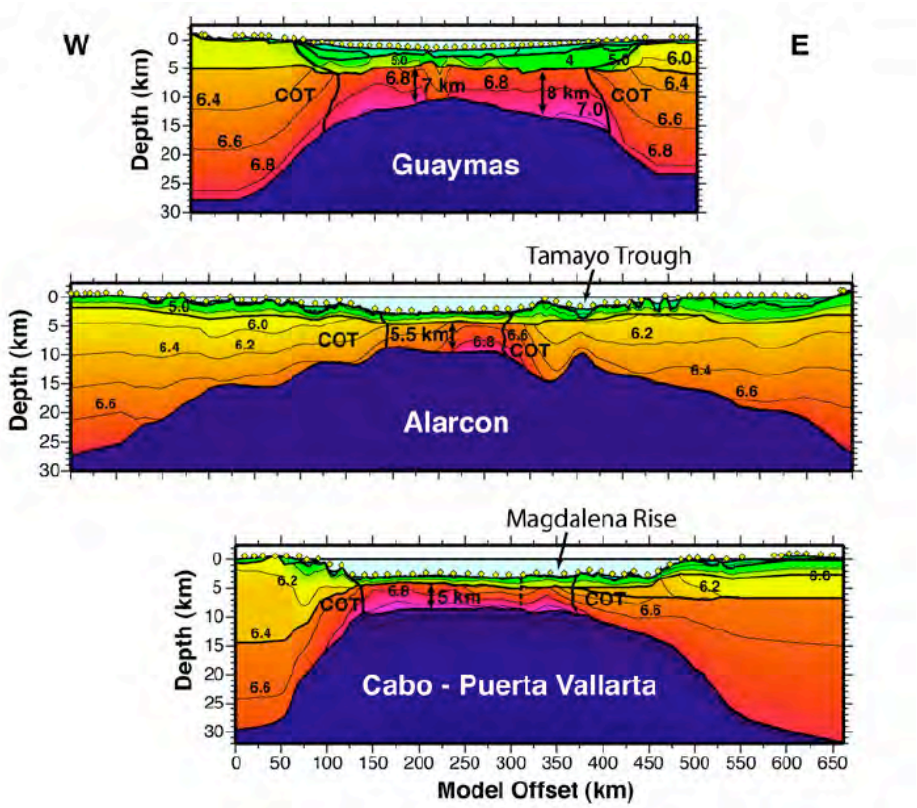

Figure 2. Models of seismic velocity structure along the Guaymas, Alarcón and Cabo-PV transects of the PESCADOR experiment. Velocity contours are labelled in km/s. Yellow diamonds are instrument locations. COT indicates interpreted continent/ocean transition. Dashed line in the Cabo-PV model indicates interpreted boundary between oceanic crust formed at the Magdalena Rise and the EPR. Models were determined using a combined forward/inverse travel time modelling approach[30]. Examples of data are presented in the Supplementary Information.

The results presented here highlight the importance of inherited mantle fertility/hydration and possibly of sediments as controlling parameters of the rifting process. The primary observations are variations in rift width and magmatism over small spatial scales, with wide, magma-poor rift segments formed over mantle that sourced voluminous pre-rift, arc magmatism, and magma-rich segments associated with thick sediments. Many rifts initiate or localize at formerly convergent boundaries in response to ridge subduction, in back-arc settings, or along suture zones following continent/continent collision. Substantial along-strike variations in the expression of rifting, with these variations controlled by pre-rift tectonics and magmatism of the formerly convergent margin, may thus be common along many rifted margins. Similarly,

Lizarralde et al 2007 *Nature*

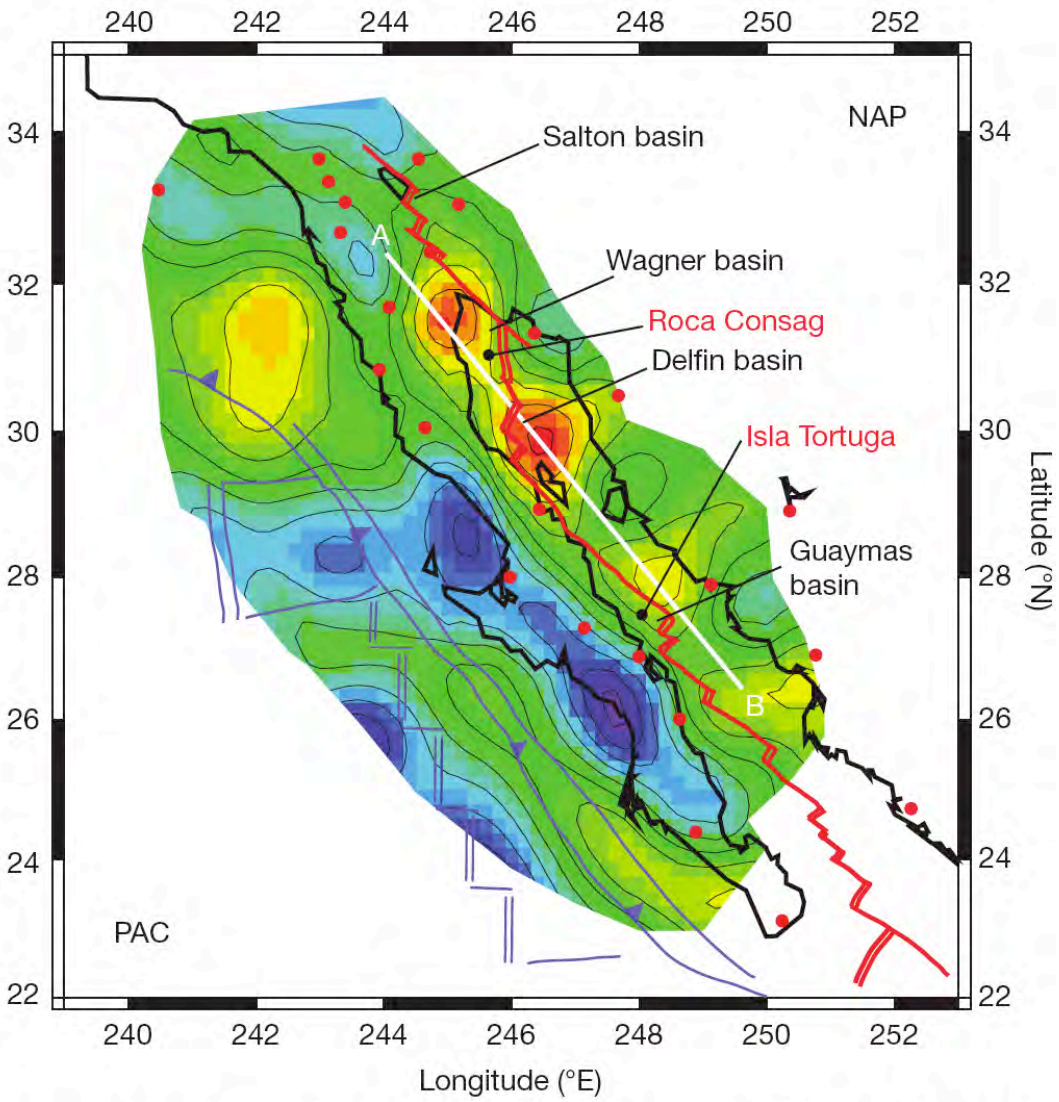

Figure 1 | Shear velocity anomalies averaged over a depth of 50 to 90 km beneath the Gulf of California and Baja California region. Negative anomalies correspond to slow regions. The contour interval is 0.5%. The coastline is indicated by the heavy black line. Red lines are the current plate boundary, with double lines indicating rifts or spreading centres and single lines indicating transform faults. Blue lines indicate the fossil spreading

Wang et al 2009 *Nature*

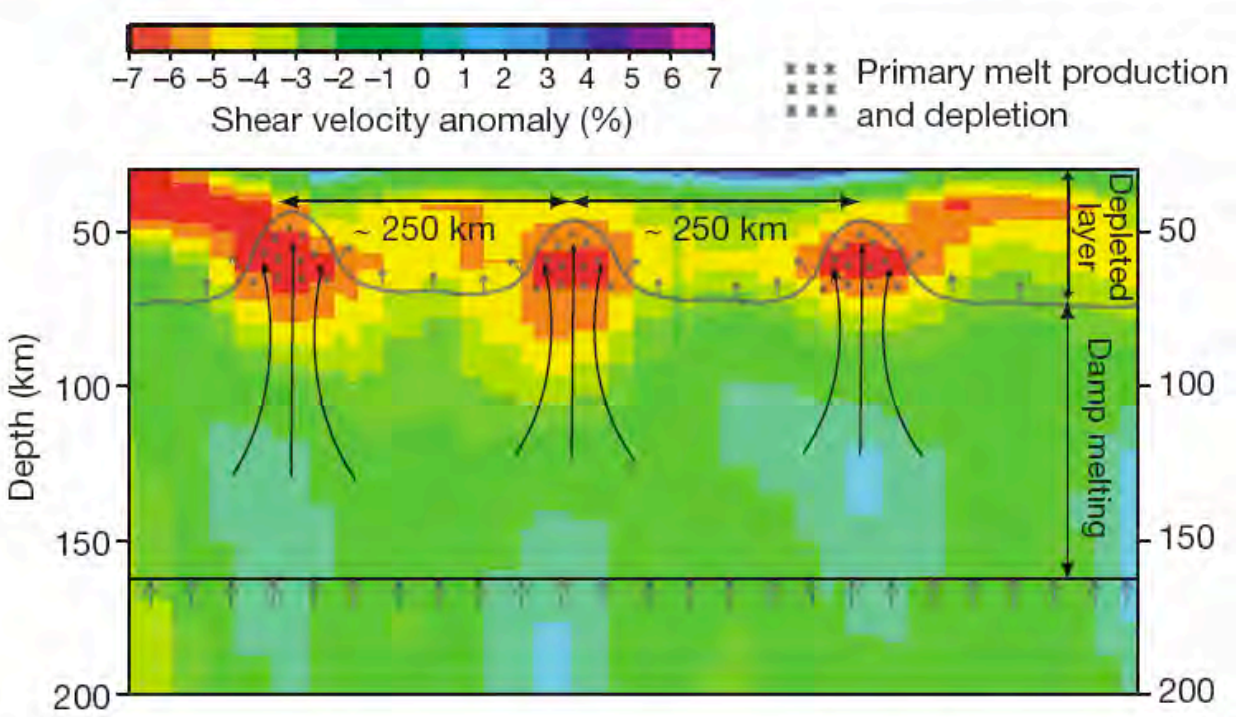

Figure 3 | Schematic interpretation of anomalous mantle velocities along profile AB. The most prominent anomalies are the low-velocity anomalies centred at depths of 60–70 km (from left to right, Wagner, Delfin and Guaymas basins), which we interpret as centres of enhanced melt concentration and upwelling. Arrows indicate directions of solid flow of the mantle matrix. Melting is assumed to begin at ~160 km in the presence of a small amount of water, leading to low S velocities (Fig. 2). Upwelling at this depth may be broadly and relatively uniformly distributed. At 60–70 km, the rate of melting is expected to increase substantially, but most of the melt is extracted, leaving a matrix that is depleted above this depth, but still containing a small melt fraction. The high-velocity anomaly near 30 km depth between the Delfin and Guaymas anomalies is due to cooling and thickening of the lithosphere with increasing age of the sea floor (see location of profile AB with respect to the spreading centres in Fig. 1).

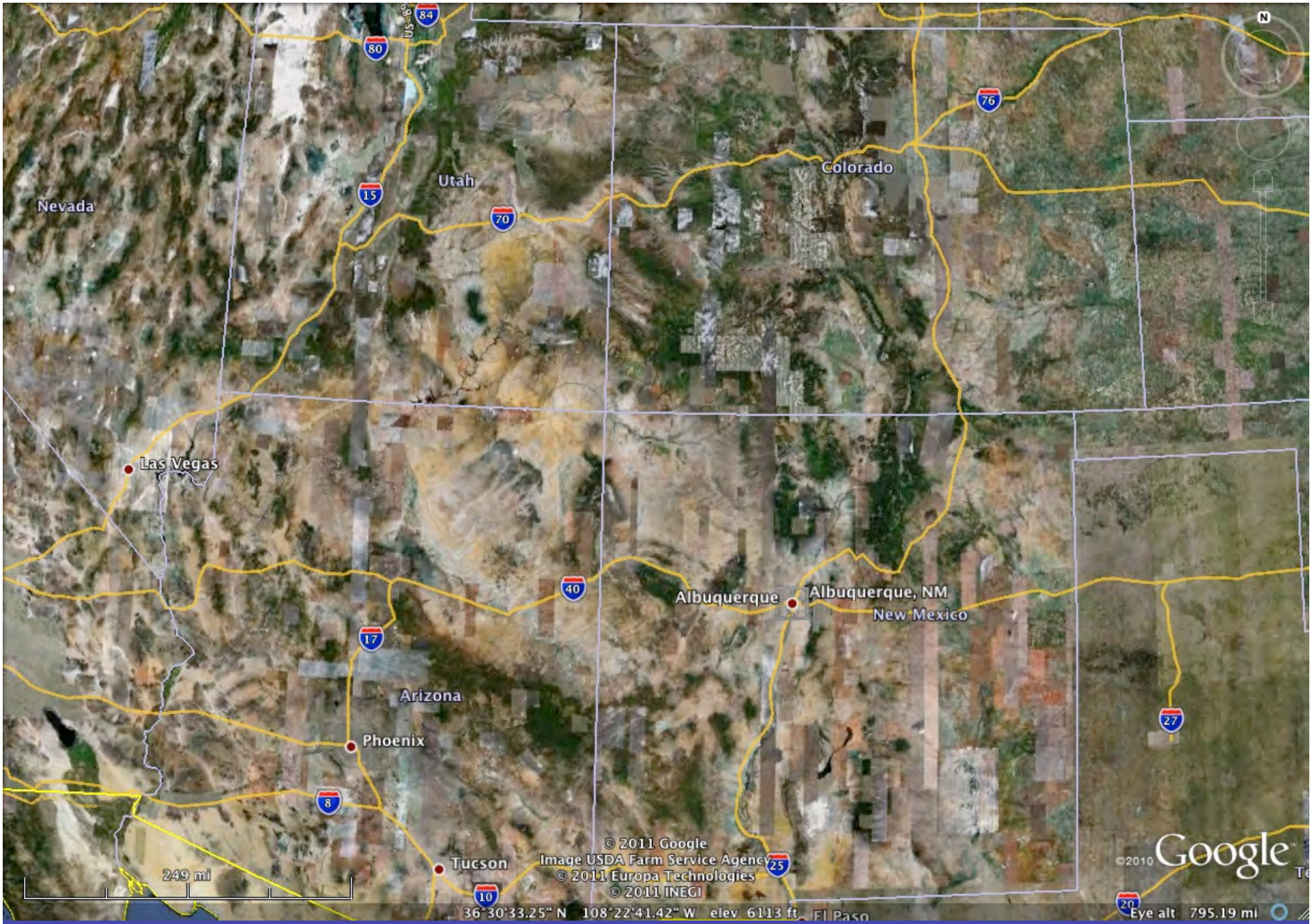
Nevada
Utah
Colorado
Las Vegas
Albuquerque
Albuquerque, NM
New Mexico
Arizona
Phoenix
Tucson
El Paso
84
80
15
70
76
40
17
8
10
25
27
20
249 mi
© 2011 Google
Image USDA Farm Service Agency
© 2011 Europa Technologies
© 2011 INEGI
36°30'33.25" N 108°22'41.42" W elev 6113 ft
©2010 Google
Eye alt 795.19 mi

ISS015E36374

El Paso, Texas, Juarez, Mexico, Franklin Mountains

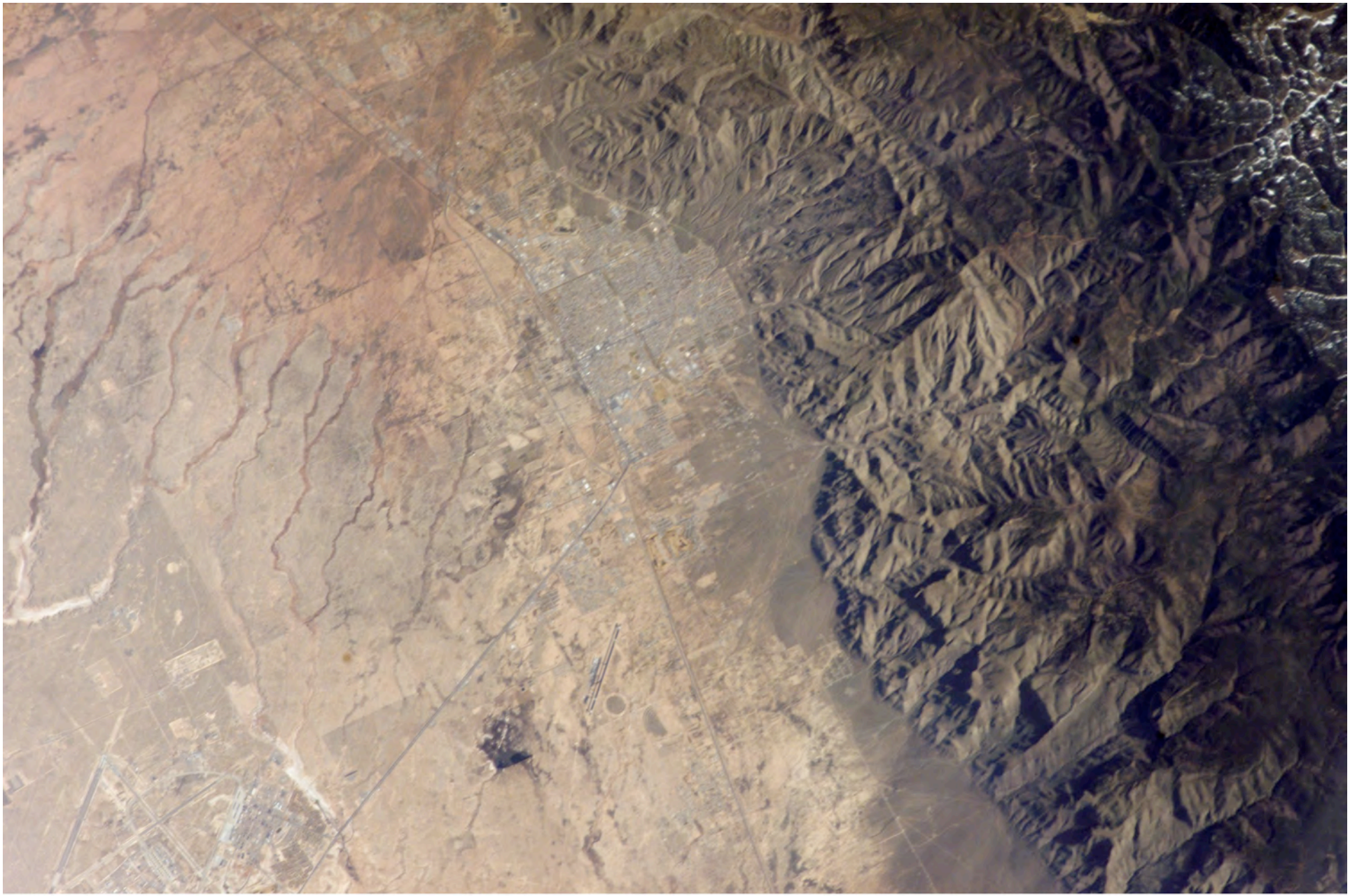

ISS004E8797

Holcomb AFB, Alamagordo, New Mexico, Sacramento Mountains

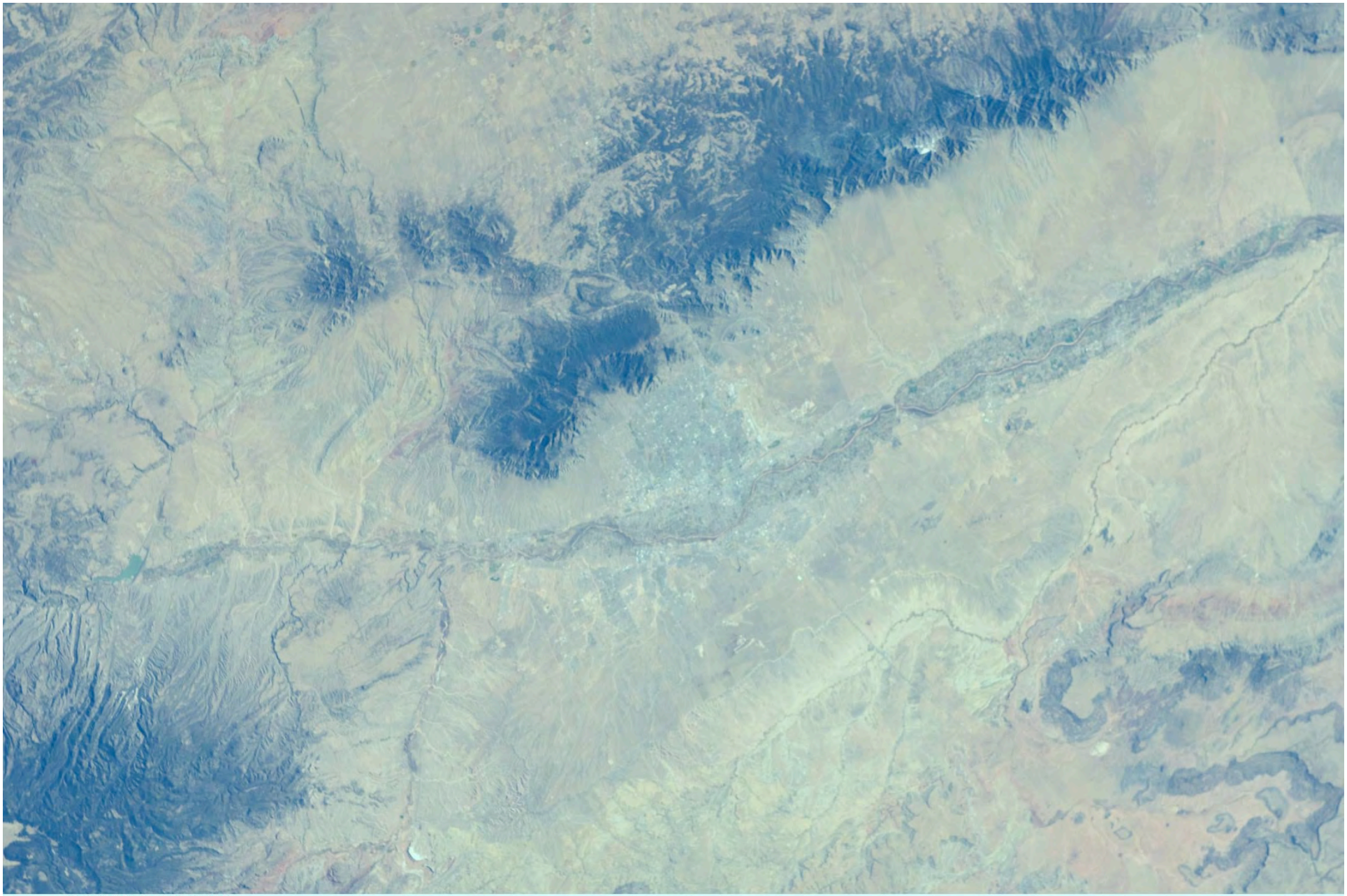

ISS025E014058

Albuquerque, New Mexico, Sandia Mountains

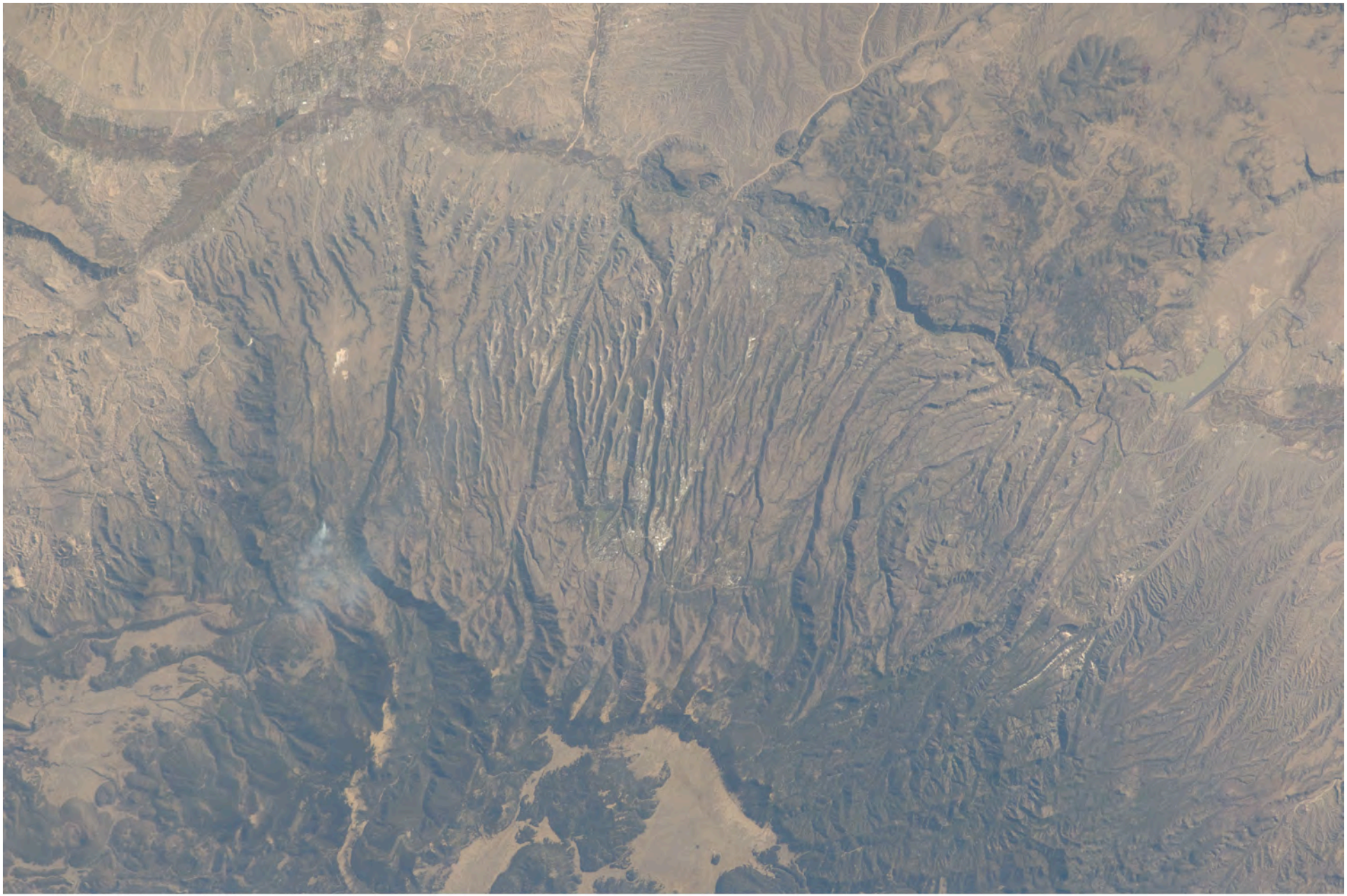

ISS018E006281

Valles Caldera, Los Alamos, Rio Grande

ISS016E006975

Taos Mountain Ski Area

ISS014E16417

San Luis Valley, Colorado

Cordell 1978
Regional
Geophysical
Setting of the
Rio Grande Rift
GSA Bulletin

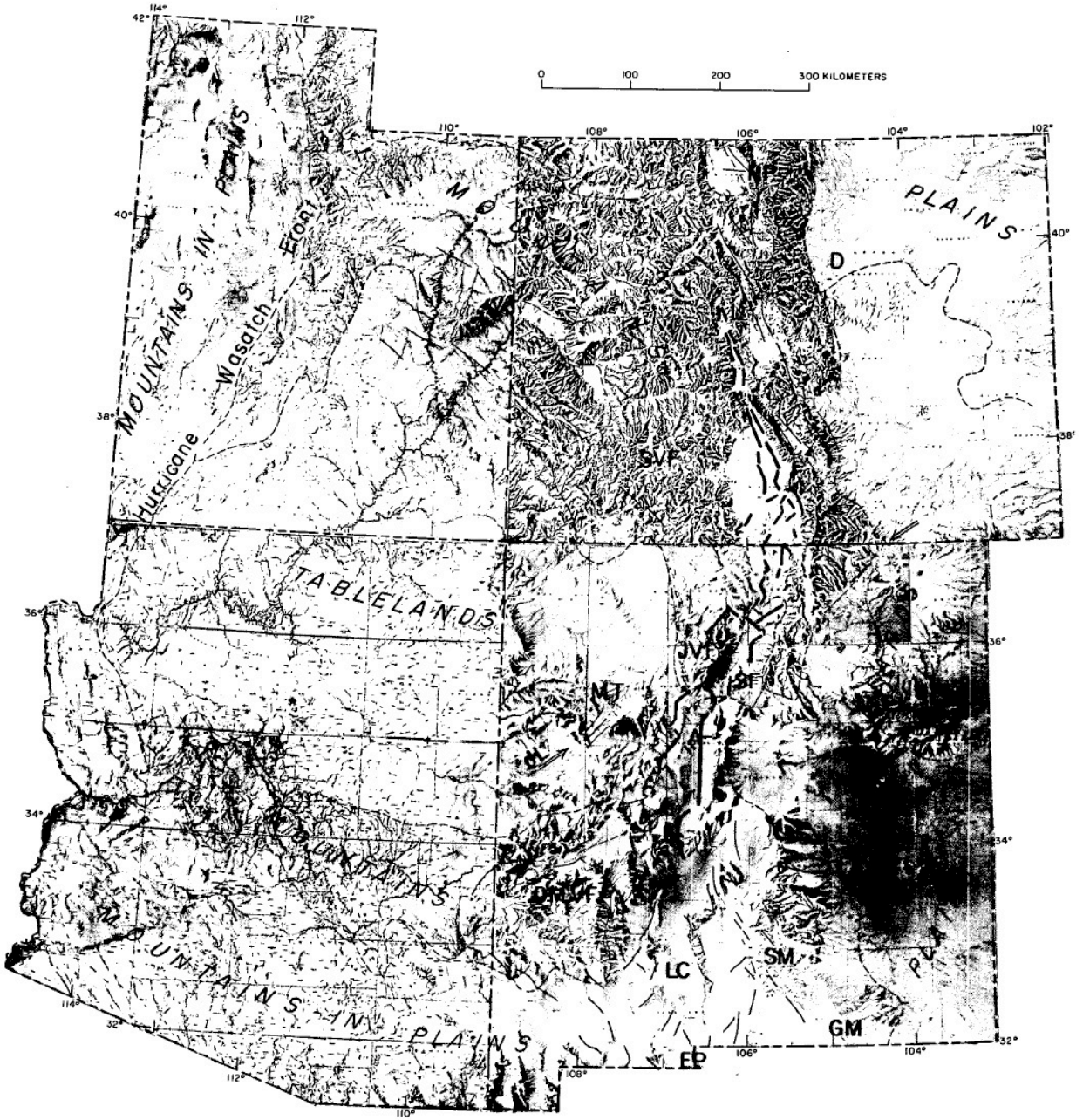

Figure 1. Locality index, major physiographic provinces (modified from Hammond, 1964), and faults of Rio Grande rift. Heavy lines show principal faults of Rio Grande graben, determined primarily from gravity data. Other faults (from Woodward, and others, 1975; Dane and Bachman, 1965; and other sources) are shown schematically with lighter lines. Base map showing Utah, Colorado, Arizona, and New Mexico modified from U.S. Geological Survey shaded relief maps, scale 1:500,000. NP = North Park, D = Denver, L = Leadville, SVF = San Juan volcanic field, JVF = Jemez volcanic field, MT = Mount Taylor, SF = Santa Fe, A = Alburquerque, JL = Jemez lineament (with arrows), S = Socorro, DMVF = Datil-Mogollon volcanic field, LC = Las Cruces, EP = El Paso, SM = Sacramento Mountains, GM = Guadalupe Mountains.

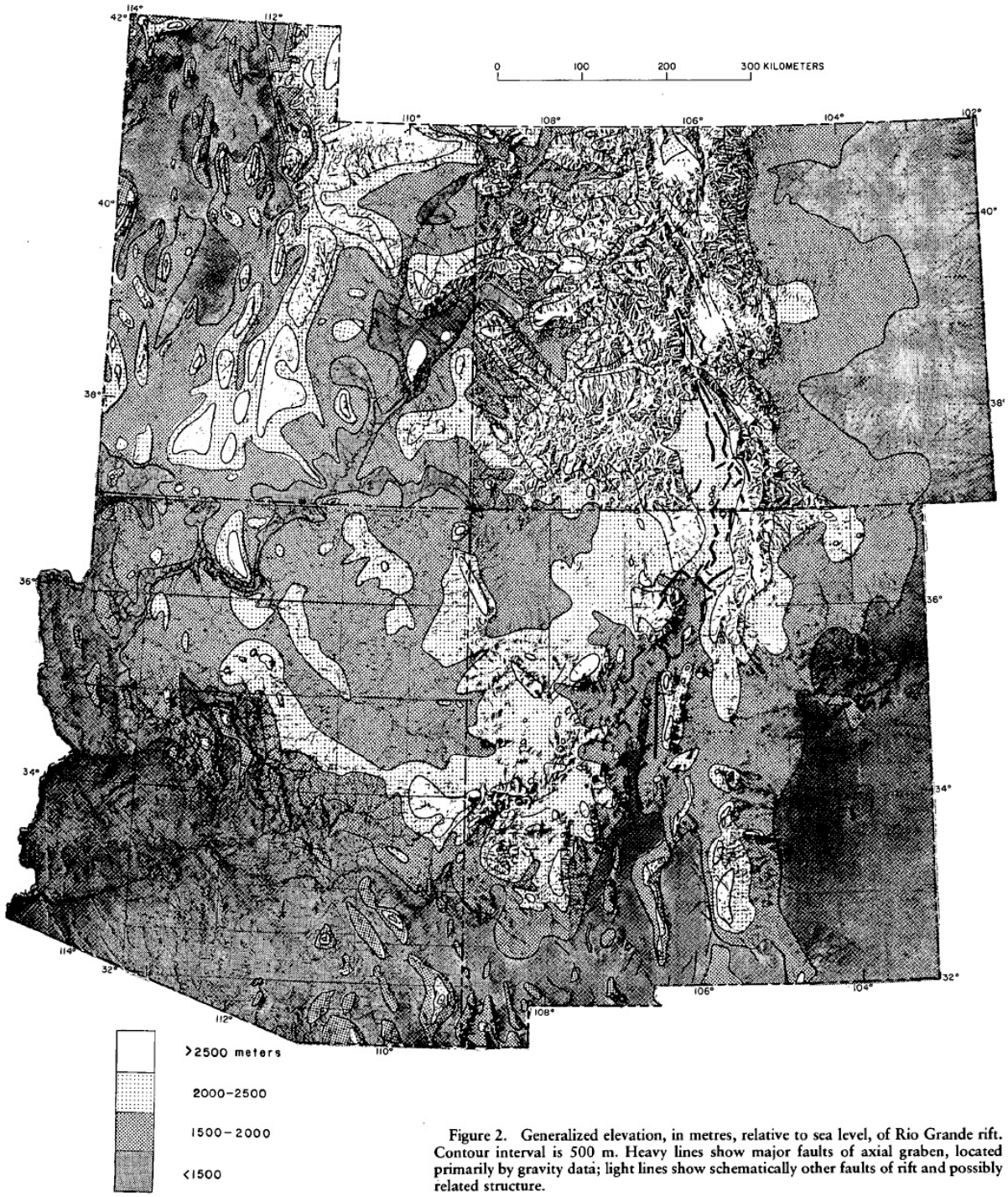

Figure 2. Generalized elevation, in metres, relative to sea level, of Rio Grande rift. Contour interval is 500 m. Heavy lines show major faults of axial graben, located primarily by gravity data; light lines show schematically other faults of rift and possibly related structure.

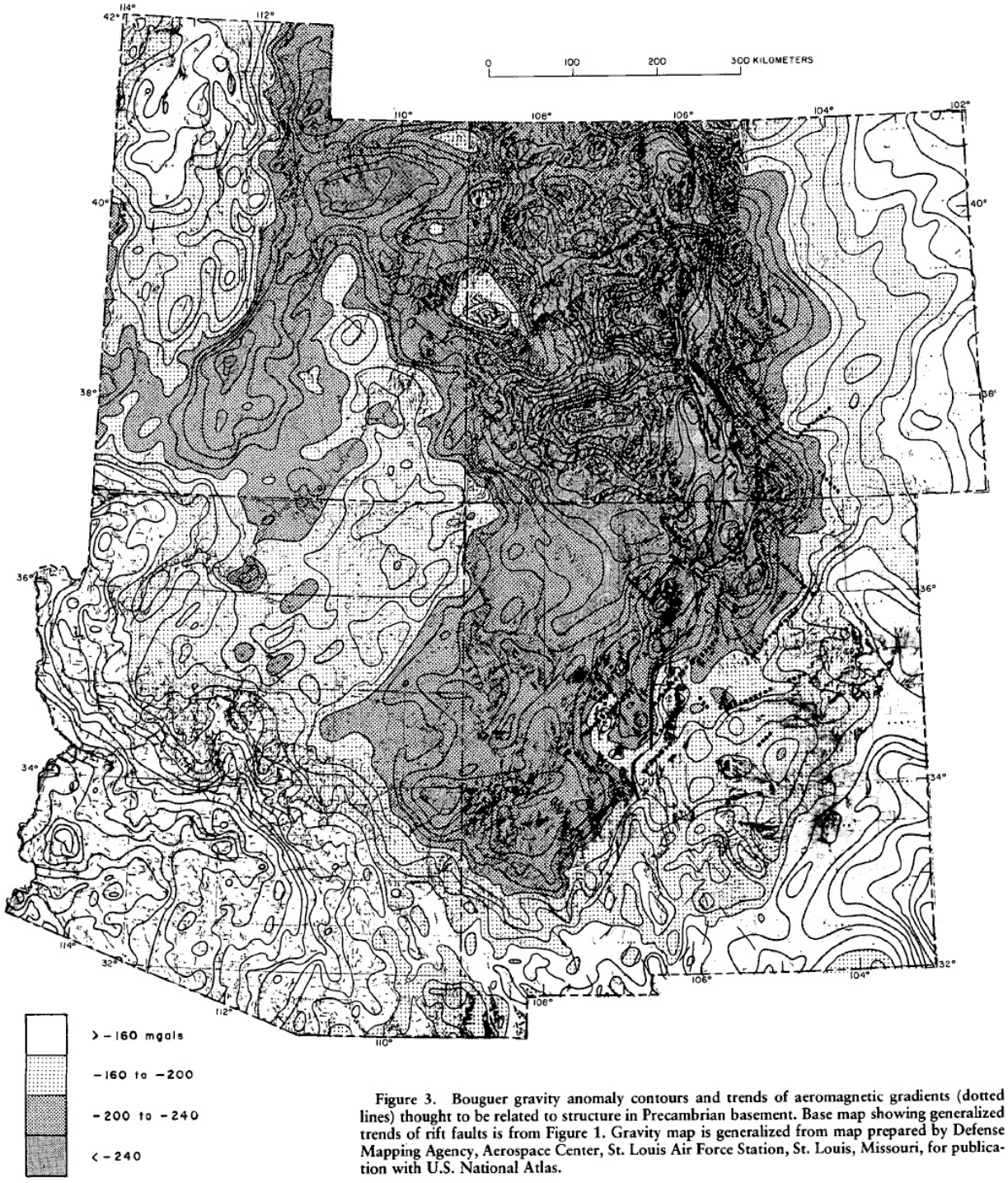

Figure 3. Bouguer gravity anomaly contours and trends of aeromagnetic gradients (dotted lines) thought to be related to structure in Precambrian basement. Base map showing generalized trends of rift faults is from Figure 1. Gravity map is generalized from map prepared by Defense Mapping Agency, Aerospace Center, St. Louis Air Force Station, St. Louis, Missouri, for publication with U.S. National Atlas.

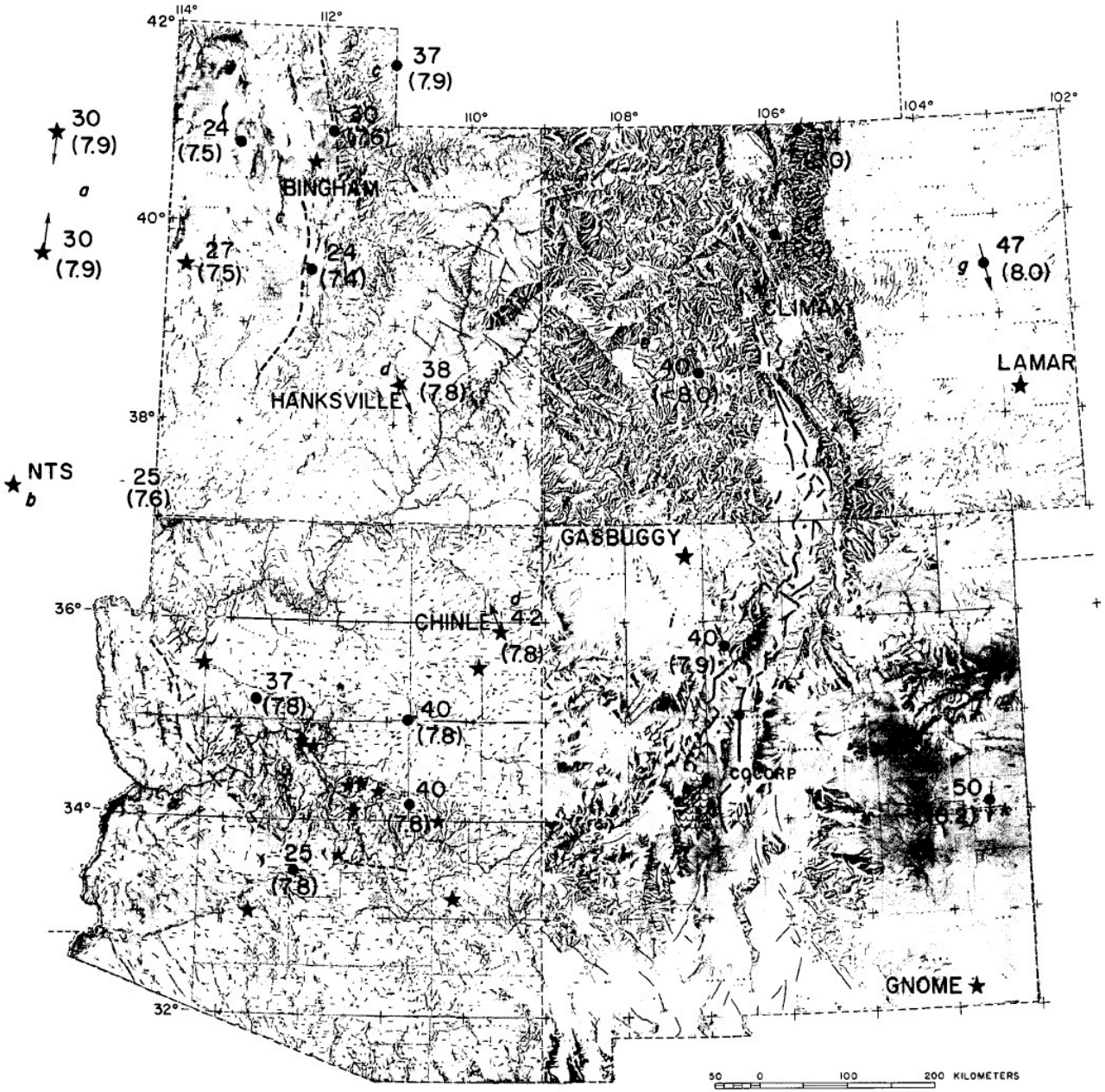

Figure 5. Seismic data, showing depth in kilometres below sea level to M discontinuity and, in parentheses, compressional wave velocity of upper mantle in kilometres per second. Stars denote shot points. Arrows at stars indicate reversed profiles; arrows at dots indicate nonreversed profiles. Location of first vibroseis profile in New Mexico by Consortium on Continental Reflection Profiling (Oliver and Kaufman, 1976) is shown by label COCORP. Recently (Kaufman and others, 1977), these profiles have been extended across western border of graben. Dashed lines show parts of western border of Colorado Plateau. Sources: a, Hill and Pakiser (1967); b, Ryall and Stuart (1963); c, Keller and others (1975) and Braile and others (1974); d, Roller (1965); e, L. Pakiser (1977, personal commun.); f, Jackson and Pakiser (1965); g, Jackson and others (1963); h, Warren (1969); i, Toppozada and Sanford (1976) and Toppozada (1974); j, crustal "low-rigidity" zone of Sanford and others (1973); k, Stewart and Pakiser (1962).

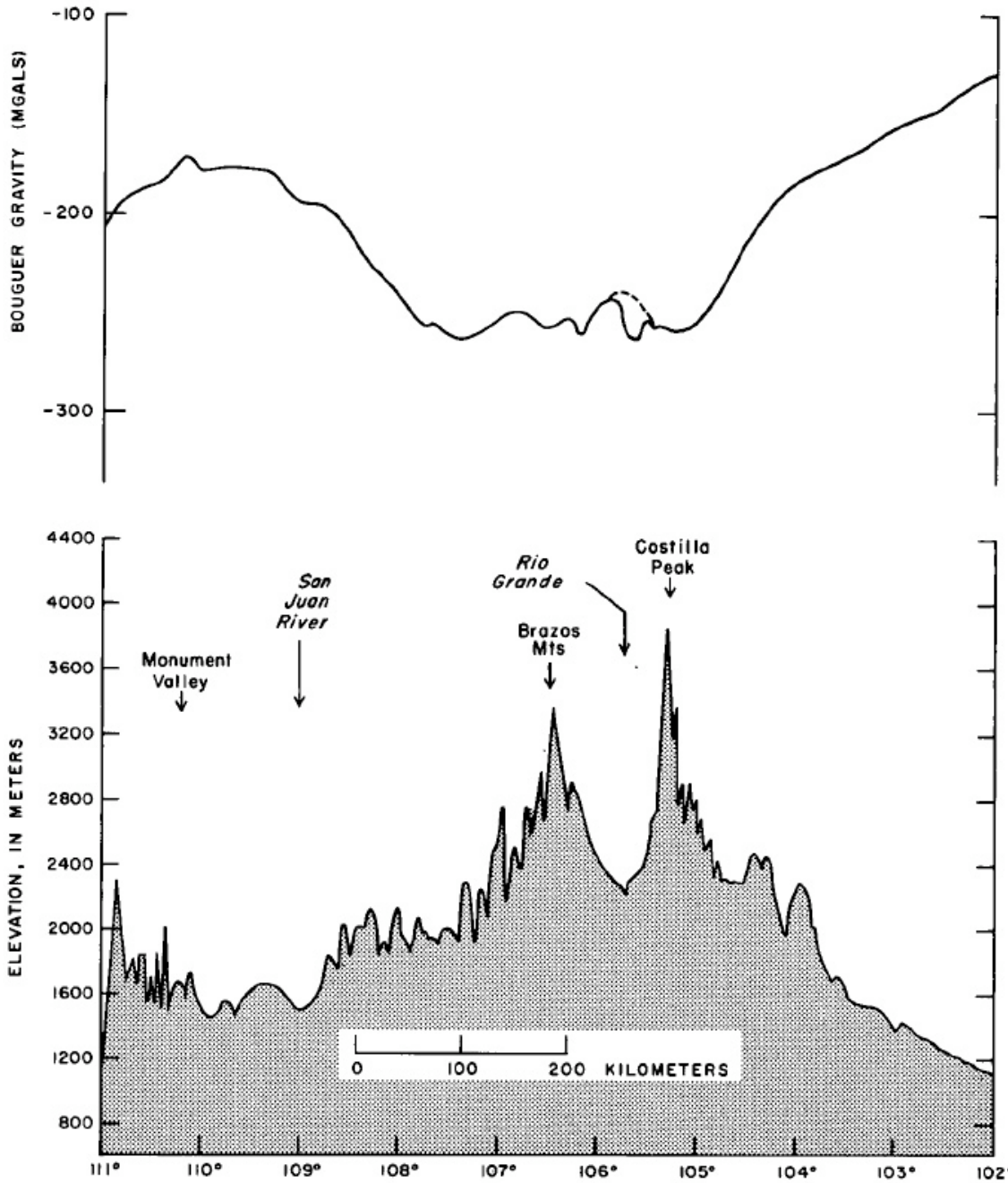

Figure 10. Gravity and elevation profiles along lat 37°N (Colorado–New Mexico border). Dashed segment of gravity profile shows, schematically, residual broad positive anomaly upon which gravity low associated with graben fill is superimposed.

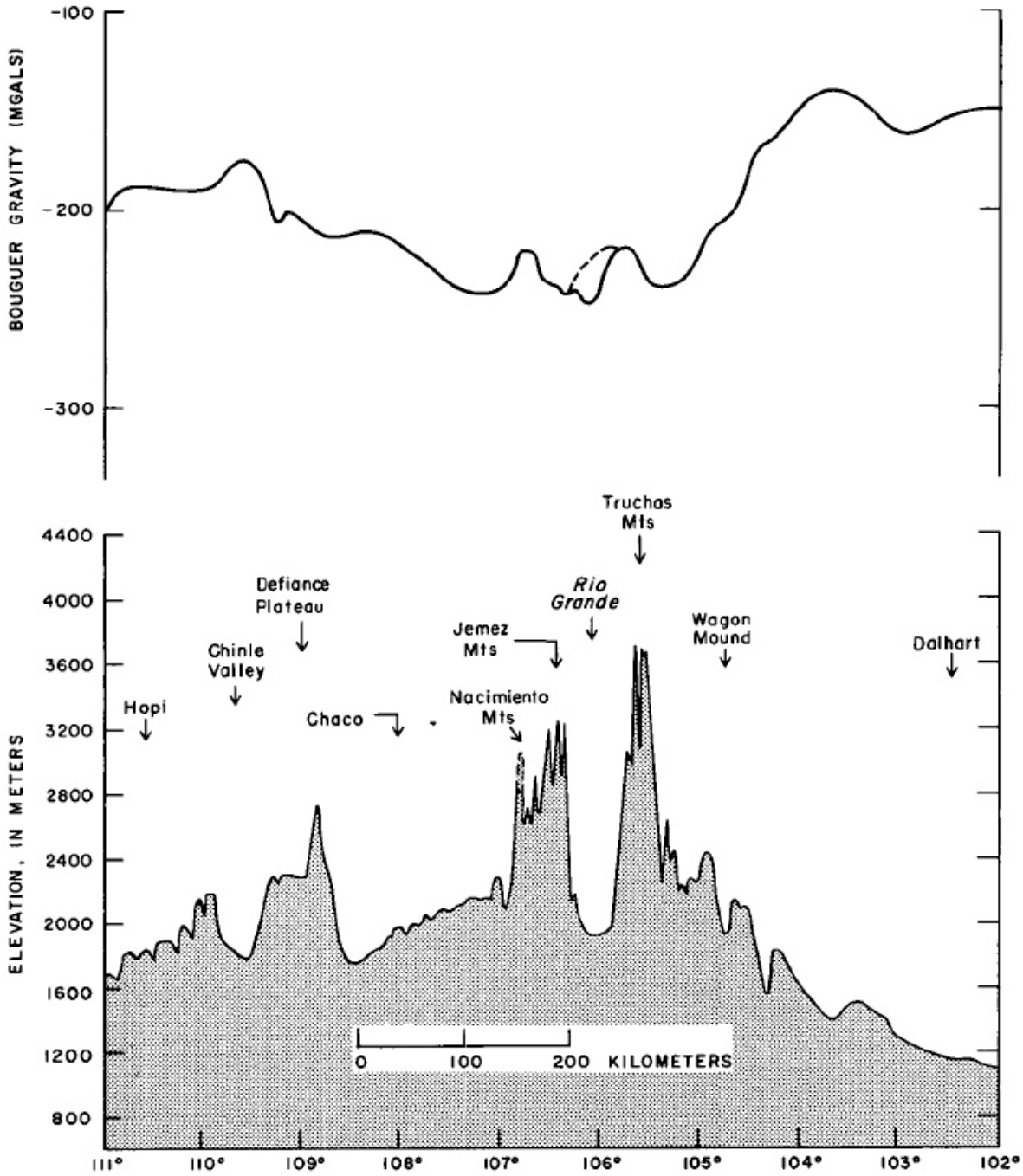

Figure 11. Gravity and elevation profiles along lat 36°N (Jemez Mountains).

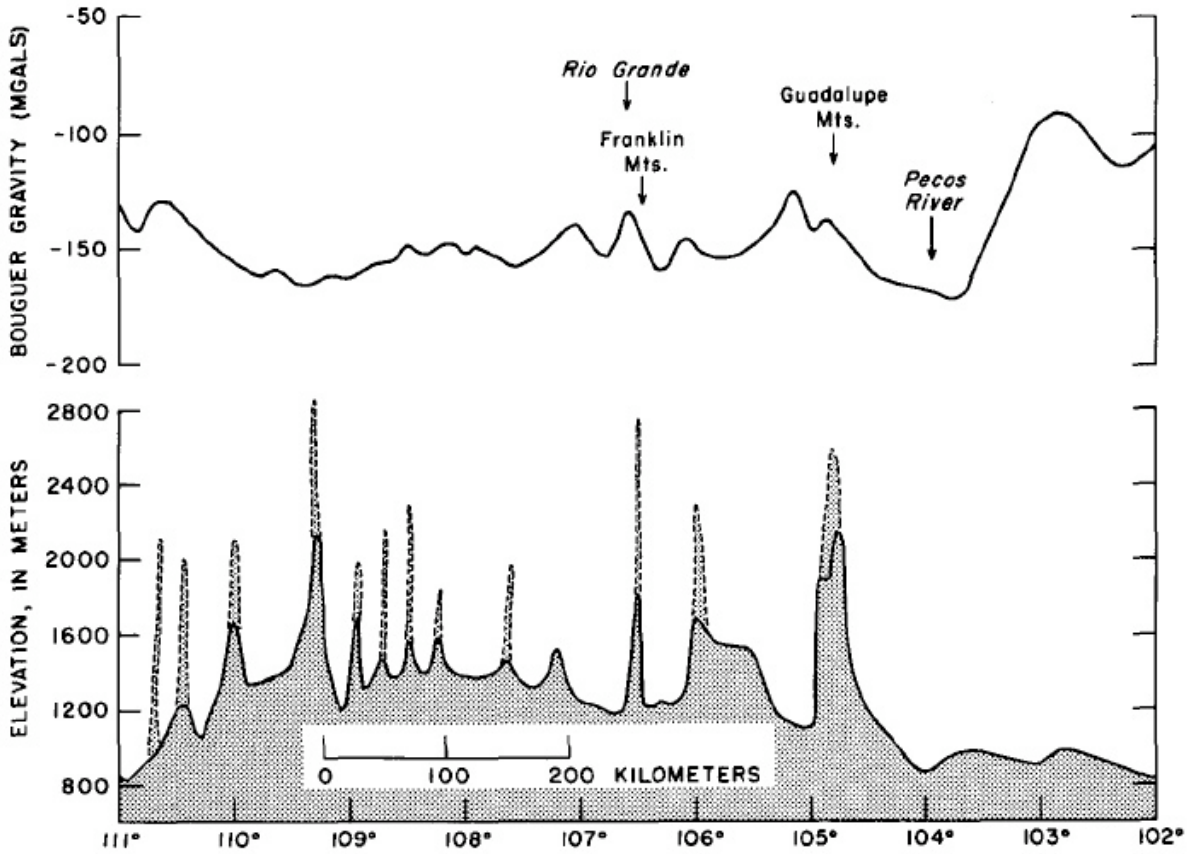

Figure 15. Gravity and elevation profiles along lat 32°N (El Paso).

The southern Rocky Mountain uplift (the Neogene-Quaternary uplift) and the Rio Grande graben cannot be considered separately. They are parts of a system of uplift, magmatism, and extension that makes up the Rio Grande rift. Among the continental rifts, a unique feature of the Rio Grande rift is its vergence, providing from south to north a sort of down-structure view of the rift process initiated as mountains and culminating as mountains-in-plains.

Zigzags in the fault blocks on the order of tens of kilometres, as well as zigzags in the trend of the rift itself on the order of hundreds of kilometres, are aligned with basement structural grain, as traced under sedimentary cover by means of the aeromagnetic data. Inherited structural grain has undoubtedly influenced both the rift and earlier uplifts along this same trend. Whether the rift has sought out a fundamental basement suture or has simply taken advantage of ubiquitous basement cracks is uncertain.

The tectonic work has been accomplished by some combination of the effects of heat, density, chemical phase change, and mass transport, all of which are interrelated. Similarly, the geophysical data — gravity, heat flow, seismic velocity, electrical conductivity, and elevation — are functionally interrelated. The system is overdetermined and, in principle, could be solved uniquely. To do so realistically would require more constraints on the geometry of deep structure within the rift itself; that is, physical-property information derived from potential-field data is reasonably complete, but sounding-type geophysical data that could provide constraints on shape and depth of critical interfaces are needed. When that information becomes available, the study of the rift will enter an exciting new phase in which the geophysical and petrological data and the geological history can be quantitatively combined.

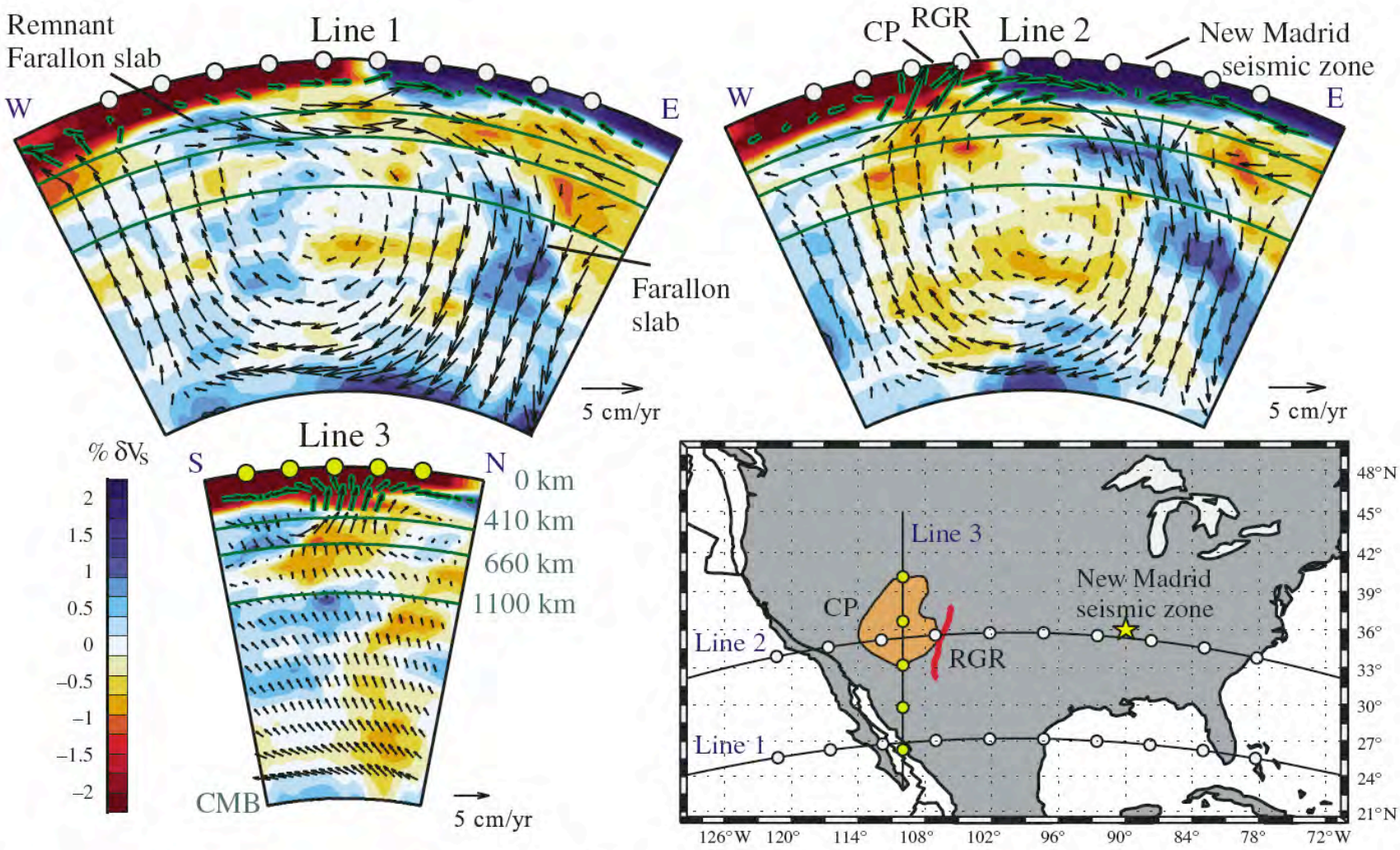

Figure 1. Calculated mantle flow (black arrows) starting at depth of 195 km beneath the U.S. in three vertical slices oriented along paths shown on map. Also shown are locations of physiographic Colorado Plateau (CP) and Rio Grande Rift (RGR). Flow is driven by density anomalies inferred from joint seismic-geodynamic modeling. Corresponding seismic tomography model is displayed in background of the slices in the form of percentage shear-wave velocity anomalies (akin to thermally induced mantle heterogeneity). CMB—core-mantle boundary.

Moucha et al 2010 *Geology*

Some of the late Cenozoic magmatic activity in the Jemez lineament, southeast of the Colorado Plateau, is thought to be of deep mantle origin (McMillan et al., 2000). Our mantle flow model portrays high upwelling velocities through a shallow thermal anomaly beneath this region. Therefore, localized melt generation through adiabatic decompression should be considered as a recent magmatic source for the Jemez lineament. Finally, to the east of the Colorado Plateau, we model a strong vertical flow that gains an eastward component and impacts the base of the lithosphere at an oblique angle directly below the Rio Grande Rift. This suggests that the upwelling flow also plays an important role in the Rio Grande Rift rifting process and leads us to propose that the Rio Grande Rift is currently active. Uncertainties in both the rates and magnitude of uplift are difficult to quantify. Qualitatively, mantle viscosity has the strongest effect on the rates of uplift, followed by uncertainties in the jointly derived tomographic model. Quantifying the uncertainties in our model on a regional scale is a topic of future study.

http://rbsc.princeton.edu/exhibitions/western/detail.php?id=22